The volume of the universe after inflation and de Sitter entropy

JHEP04(2009)118

(http://iopscience.iop.org/1126-6708/2009/04/118)

Published by IOP Publishing for SISSA
Received: *February 4, 2009*
Accepted: *April 13, 2009*
Published: *April 28, 2009*

The volume of the universe after inflation and de Sitter entropy

Sergei Dubovsky,[a,b] **Leonardo Senatore,**[c,d,e] **and Giovanni Villadoro**[f]

[a] *Department of Physics, Stanford University, Stanford, CA 94305, U.S.A.*
[b] *Institute for Nuclear Research of the Russian Academy of Sciences, 60th October Anniversary Prospect, 7a, 117312 Moscow, Russia*
[c] *School of Natural Sciences, Institute for Advanced Study, Olden Lane, Princeton, NJ 08540, U.S.A.*
[d] *Jefferson Physical Laboratory, Harvard University, Cambridge, MA 02138, U.S.A.*
[e] *Center for Astrophysics, Harvard University, Cambridge, MA 02138, U.S.A.*
[f] *CERN, Theory Division, CH-1211 Geneva 23, Switzerland*
E-mail: dubovsky@stanford.edu, senatore@physics.harvard.edu, giovanni.villadoro@cern.ch

Abstract: We calculate the probability distribution for the volume of the Universe after slow-roll inflation both in the eternal and in the non-eternal regime. Far from the eternal regime the probability distribution for the number of e-foldings, defined as one third of the logarithm of the volume, is sharply peaked around the number of e-foldings of the classical inflaton trajectory. At the transition to the eternal regime this probability is still peaked (with the width of order one e-folding) around the average, which gets twice larger at the transition point. As one enters the eternal regime the probability for the volume to be finite rapidly becomes exponentially small. In addition to developing techniques to study eternal inflation, our results allow us to establish the quantum generalization of a recently proposed bound on the number of e-foldings in the non-eternal regime: the probability for slow-roll inflation to produce a finite volume larger than $e^{S_{\rm dS}/2}$, where $S_{\rm dS}$ is the de Sitter entropy at the end of the inflationary stage, is smaller than the uncertainty due to non-perturbative quantum gravity effects. The existence of such a bound provides a consistency check for the idea of de Sitter complementarity.

Keywords: Cosmology of Theories beyond the SM, Models of Quantum Gravity, Space-Time Symmetries, Spacetime Singularities

ArXiv ePrint: 0812.2246

doi:10.1088/1126-6708/2009/04/118

JHEP04(2009)118

Contents

JHEP04(2009)118

1 Introduction

The Universe is accelerating today [1–3], and it is extremely likely that it was experiencing a period of accelerated expansion (inflation) back in the past [3–6]. In both cases the pressure to density ratio is very close to -1 and the local geometry is very close to that of de Sitter (dS) space.

It is plausible that both these periods of inflation are eternal, i.e. some space-time regions keep inflating forever. Indeed the most economical explanation for the cosmic acceleration observed now is that we are stuck in a metastable vacuum [7], and this results in eternal inflation unless the vacuum decay rate Γ is faster than the expansion rate of the Universe, $\Gamma \gtrsim H_0$.[1] Also there is strong evidence that in the past we underwent a phase of inflation driven by a rolling scalar field, which could have been preceeded by a period of eternal inflation, as predicted in many field theoretical models [9–11]. Further, the current picture of the string landscape [12] suggests that the observed part of the Universe was created as a result of tunneling from some higher-scale eternally-inflating vacuum [13]. All these arguments make the study of eternal inflation very important.

[1] This latter possibility appears rather unlikely and fine-tuned given the non-perturbative nature of the decay, although it may receive support from future particle physics data [8].

Moreover eternal inflation provides a natural framework to implement Weinberg's solution of the cosmological constant problem [14], which is the most plausible so far in spite of the many efforts made to find an alternative. According to this solution the choice of the vacuum is made, at least partially, by anthropic reasons such as the requirement that structures were able to form in our Universe. These arguments raise the notoriously difficult and puzzling question of making predictions in an eternally inflating Universe.

On a purely practical side we possess a well developed machinery of quantum field theory in curved space-time that proved to be very successful in calculating properties of the primordial density perturbations with many fine details in the case of non-eternal inflation (see e.g. [15]). The applications of these techniques to the case of eternal inflation is instead much more challenging, as in this latter regime the size of the quantum fluctuations is large, a non-perturbative treatment is required and calculations become in general much more difficult (see e.g. [16] for a recent discussion). On the other hand, without a clear understanding of the eternally inflating geometry, it might be hopeless to solve the issues raised by eternal inflation such as the measure problem in the landscape; this is why we find it very important to make explicit and precise calculations in this regime.

On a more theoretical side, dS space appears to share many properties with the black hole geometry — most importantly, in both space-times the most natural sets of observers (the asymptotic observers in the black hole case and the comoving ones in the accelerating Universe) see a gravitational horizon with the associated thermodynamic properties, such as Hawking temperature and Bekenstein entropy, the latter, in the case of de Sitter, being equal to [17]

$$S_{\rm dS} = \pi \frac{M_{\rm Pl}^2}{H^2} \,,$$

where $M_{\rm Pl}^2 \equiv 1/G_N$ with G_N the Newton constant. A finite entropy suggests that the system is described by a finite number of degrees of freedom, or more formally, the Hilbert space describing the system at the quantum level has a finite dimensionality equal to $e^{S_{\rm dS}}$. It is widely believed that both black holes and de Sitter space always arise as a subsector of a larger theory with an infinite dimensional Hilbert space. This is obvious for a black hole in asymptotically Minkowski or adS space-times, but less clear for dS space. Indeed, in principle one could imagine a quantum gravity theory with, for example, a single positive energy vacuum. However, this is not the case in the known string theory landscape [18] and there are general arguments strongly suggesting that dS vacua are always metastable with respect to decay to either the Minkowski or the adS minima of the potential [19]. This will be the point of view adopted in the current paper and by dimensionality of the Hilbert space describing black hole or dS space we always understand the dimensionality of the corresponding subsector in a larger, most likely infinite-dimensional, Hilbert space (although, it is worth noting that an alternative line of thought is also being pursued [20]).

Taking seriously the similarity between the causal structures of de Sitter and Schwarzschild causes a serious doubt on the validity of the global semiclassical picture of the eternally inflating Universe.[2] Indeed, the remarkable fact about black holes is that the

[2]This idea is being pursued by a number of authors, see e.g., [21]. Our discussion mainly follows that of [22].

JHEP04(2009)118

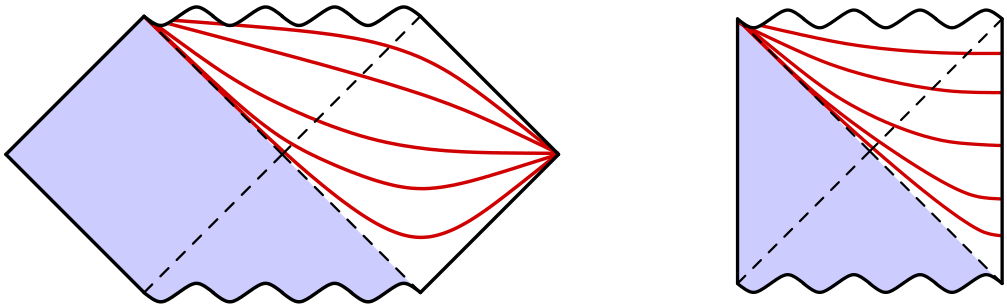

Figure 1. Set of space-like slices covering both the exterior and the interior of: a) a black hole (left) and b) an eternal inflating universe (right).

JHEP04(2009)118

global effective field theory description of the space-time claiming to describe both the interior and the exterior of the horizon eventually breaks down (see e.g. [23]).

More concretely, if one considers the set of space-like slices covering both the exterior and the interior of a black hole, as shown in figure 1a, and insists that the field theory description is valid on this set of slices, one comes to the conclusion that the information is lost in the course of the black hole evaporation [24]. This conclusion was proven to be wrong [25, 26] by the adS/CFT correspondence that provides a description of the system involving black holes (gravity in the bulk adS space) in terms of an unitary boundary CFT. Consequently, one is forced to conclude that the global effective field theory description breaks down at the time scale of order the evaporation time, $t \sim R_s^3/G_N$, where R_s is the Schwarzschild radius and G_N the Newton constant (for a recent review see for example [22]). After this time the information about the inside observer gets reprocessed in the evaporating Hawking quanta, and by insisting on a simultaneous local description of the exterior and the interior on longer time-scales one would run into a contradiction with the "no quantum xerox" principle (or equivalently with the linearity of quantum mechanics) [27, 28]. This conclusion is really surprising given that one can always choose a set of slices that avoid the region close to the singularity, so that naively one would expect the effective field theory to hold.

Given the similarity between the causal structures of de Sitter space and that of Schwarzschild geometry, one may suggest that also in dS space the global description in terms of a similar set of slices (shown in figure 1b) eventually breaks down. Note that these slices are just the conventional FRW slices that are commonly used to describe the inflationary Universe. Going on with the analogy with the black holes one expects this breakdown to happen at a time-scale of order $t \sim H^{-3}/G_N$ or, equivalently, after a period of order $S_{\rm dS}$ e-foldings. One may expect that space-time events outside the region containing $e^{S_{\rm dS}}$ Hubble patches get encoded in de Sitter fluctuations, similarly to how the information inside the black hole gets released in the Hawking quanta after the evaporation time.

Note that, unlike in the black hole case, we are not running into any paradox if this does not happen, therefore it may well be that pushing the analogy this far is too naive.

However, if one takes it seriously there is an immediate test to pass. Indeed, in the black hole case, due to the presence of a curvature singularity, it is impossible to read the information in the Hawking quanta and then jump into the black hole and read the same information again. Similarly, it should not be possible to get the same information twice in the de Sitter case as well.

However, if inflation could last for an arbitrarily long time without becoming eternal, an observer would be able to first read the information in the dS fluctuations and later, as more and more space-time becomes visible after inflation, he would be able to access it directly. Consequently, for the above ideas about de Sitter complementarity to be consistent, there should be a limit on how long inflation can last without becoming eternal [22],

$$3N \leq cS_{\rm dS} \ , \tag{1.1}$$

where N is the number of e-foldings (defined as one third of the logarithm of the total volume after inflation) and c is a coefficient of order one. On the other hand, no limit on the number of e-foldings is required on those realization that are eternal, because in those cases the observer is not able to access all the volume after reheating.

It was proven in [22] that the bound (1.1) indeed holds for the classical inflaton trajectory in any theory of inflation that does not allow violations of the null energy condition,

$$\rho + p \geq 0 \ ,$$

where ρ and p are the energy density and the pressure. On the other hand, violation of the bound (1.1) is possible in theories able to violate the null-energy condition, such as ghost inflation [29]. This is actually encouraging and supports arguments establishing the link between horizon complementarity and duration of inflation, as also the conventional black hole thermodynamics breaks down in theories where the null energy condition can be violated [30, 31].

There are two reasons leading to an uncertainty in the numerical value of the coefficient c in the bound (1.1) as proven in [22]. First, at the time when the bound was proposed the exact condition for inflation to become eternal was unknown, and it was not even clear whether there is a sharp distinction between eternal and non-eternal regimes. This issue was addressed in [16] and the conclusion is that there is a sharp transition between these two regimes, with the condition not to have eternal inflation being

$$\Omega \equiv \frac{2\pi^2}{3}\frac{\dot{\phi}^2}{H^4} \geq 1 \ , \tag{1.2}$$

where $\dot{\phi}$ is the classical velocity of the inflaton field.

Now it is straightforward to find a bound on the number of e-foldings for the classical inflaton trajectory in single-field slow-roll inflation in the non-eternal regime. Namely, one writes

$$\frac{dS_{\rm dS}}{dN_c} \equiv \frac{M_{\rm Pl}^2 dH^{-2}}{H dt} = -\frac{2M_{\rm Pl}^2 \dot{H}}{H^4} = 12\Omega \ , \tag{1.3}$$

where at the last step we made use of the second Friedmann equation. By integrating (1.3) and using the condition (1.2) for the absence of eternal inflation we obtain (1.1) with the

JHEP04(2009)118

value $c = 1/4$,

$$3N_c \leq \frac{S_{\rm dS}}{4} \,, \tag{1.4}$$

where N_c is the number of e-foldings on the classical inflaton trajectory.

However, this does not establish the sharp version of the bound (1.1) yet. There is another reason for the uncertainty in the bound (1.1). Namely, the above analysis (and that of [22]) is restricted to the classical inflaton trajectory. This approximation clearly breaks down when Ω is of order (but still larger than) one, so that inflation is close to be eternal. In this case, even though inflation is not eternal, the typical inflaton trajectory is very different from the classical one and can be much longer. More generally, at the quantum level for any value of Ω there is always a non-vanishing probability for the actual inflaton trajectory to be long enough to violate the bound (1.1) for any value of c.

In this situation it is natural to study what is the probability distribution for inflaton trajectories of different lengths — in other words, what is the probability distribution for the volume of the Universe $\rho(V)$ after inflation. It is not clear a priori what the natural generalization of the bound (1.1) should look like at the quantum level. One might expect that there exists a value of c such that the probability to violate (1.1) is suppressed, for example as non-perturbative quantum gravity effects $e^{-S_{\rm dS}}$ (which would correspond to $\rho(V) \sim 1/V^{\alpha}$) or even more, for example exponentially with the volume $\rho(V) \sim e^{-V}$ (which would correspond to order $e^{-e^{S_{\rm dS}}}$ effects). What we find from our analysis is that such value of c exists (it is $c = 1/2$) and that the probability associated to the violation of the bound is actually super-exponentially small, i.e. $\sim e^{-e^{S_{\rm dS}}}$.

To achieve this goal we obtained another result of independent interest. Namely, we calculated in an explicit form the probability distribution for the volume of the Universe after slow-roll inflation $\rho(V)$ both in eternal and non-eternal regimes. This offers further insight in the actual geometry of the eternally inflating spacetime. While, unlike the density perturbation spectrum, this quantity is not of much interest for current observations, it still appears to be one of the natural "theoretical" observables to look at in the study of eternally inflating Universes. In particular, according to [16], the order parameter for the transition to eternal inflation is the normalization of $\rho(V)$,

$$P_{\rm ext} = \int_0^\infty dV \rho(V) \,. \tag{1.5}$$

At $\Omega > 1$ this quantity is equal to 1, in agreement with the naive expectation. However, at $\Omega < 1$ the normalization $P_{\rm ext}$ becomes smaller then 1, indicating that there is a non-zero probability $(1 - P_{\rm ext})$ for the reheating volume to be infinite, i.e. for inflation to last forever. In this paper we will rederive this result in yet another, somewhat more explicit, way. It is also worth noting that recently the far exponential tail of the probability $\rho(V)$ was calculated in [32] in the eternal regime. This result was used there to define a "reheating-volume" measure for observables after eternal inflation. It appears that the explicit expression for $\rho(V)$ has good chances to be useful in further theoretical studies of de Sitter space and eternal inflation.

The rest of the paper is organized as follows. We start section 2 with a review of the discrete stochastic branching process introduced in [16] to describe inflation. Then

JHEP04(2009)118

we use this model to derive a differential equation (2.22) for the Laplace transform of the probability distribution $\rho(V)$. Similar discrete models were used in [33] and they are essentially equivalent to the stochastic description of inflation by Starobinsky [34]. Within the stochastic approach equation (2.22) is known as the "non-linear Fokker–Planck equation" [35].

In section 3 we provide approximate solutions for the equation (2.22) and calculate the probability distribution in different regimes. We start with a discussion of the general properties of the solutions of (2.22), and rederive in a new and very explicit way that $\Omega = 1$ is the transition point to the eternally inflating regime, *i.e* that $P_{\rm ext} = 1$ for $\Omega > 1$ and $P_{\rm ext} < 1$ for $\Omega < 1$. Then in section 3.1 we study the moments of the volume distribution. We show that there is a simple way of calculating them without actually solving equation (2.22) and performing the Laplace transform. In agreement with the results of [16] we prove that at $\Omega > 1$ sufficiently high moments diverge for any value of Ω if the inflaton field is allowed to take arbitrarily high values. We find the values Ω_n such that the n-th moment diverges at $\Omega < \Omega_n$, and illustrate our method by explicitly calculating the average and the variance.

In section 3.2 we start analyzing the properties of the probability distribution by performing the Laplace transform. First, we consider the semiclassical limit $\Omega \gg 1$, and find an approximate solution for eq. (2.22) in this limit. It turns out that because of the non-commutativity of the large-volume and the large-Ω limits this solution does not capture correctly the large volume tail of the probability distribution where the probability becomes smaller than $\sim e^{-\Omega}$. The study of this solution is also instructive for developing an intuition on how to perform the Laplace transform of the solutions of eq. (2.22). In section 3.3 we apply this intuition for general $\Omega > 1$, when it is not possible to find an approximate solution to (2.22) in closed form. By solving this equation in different regimes one can obtain enough information to reconstruct the probability distribution in the physically relevant case $N \gg 1$. $\rho(V)$ turns out to be peaked around the average value

$$\overline{N} = \frac{2N_c}{1+\sqrt{1-\Omega^{-1}}} \,. \tag{1.6}$$

For $N < \overline{N}$ it takes the following Gaussian form

$$\rho(N) \simeq \mathcal{N} e^{-\frac{(3N-3\overline{N})^2}{2\sigma^2}} \,, \qquad \Omega > 1 \tag{1.7}$$

where the width σ is equal to

$$\sigma^2 = \frac{2}{\Omega(1+\sqrt{1-\Omega^{-1}})^2} \,. \tag{1.8}$$

As Ω approaches the transition point, $\Omega = 1$, the width σ becomes of order one, which is still narrow in the regime of large number of e-foldings, $N \gg 1$, the one we are interested in. So the most important consequence of the change of Ω is that the average number of e-foldings $\overline{N}$ changes. In agreement with the naive expectation it increases as Ω approaches the transition point, but it does not grow a lot: at $\Omega = 1$ the average number of e-foldings is twice as large as the classical one.

JHEP04(2009)118

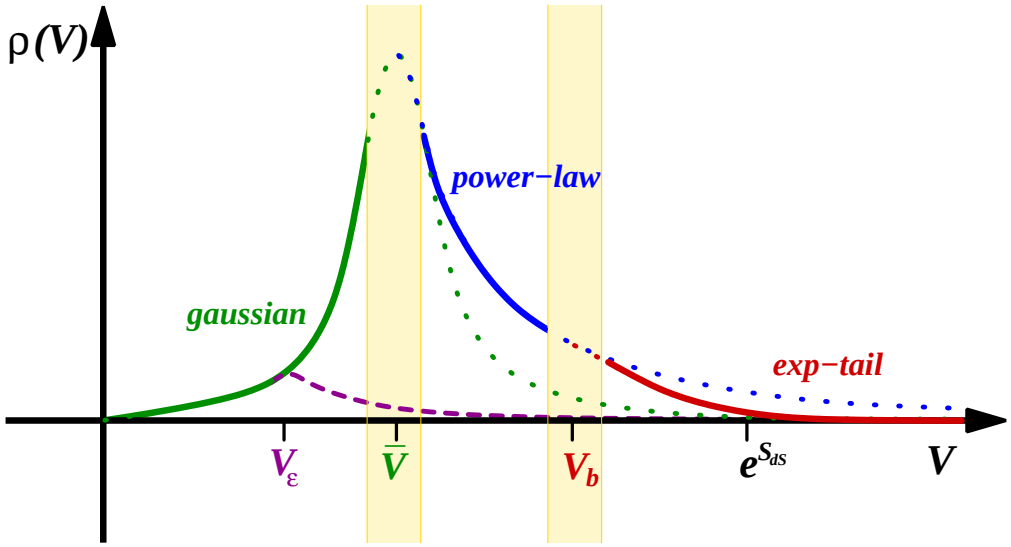

Figure 2. Typical shape for the probability distribution of the volume $\rho(V)$. For small volumes the behavior is gaussian with the number of e-foldings ($\rho \sim e^{-c(N-\overline{N})^2}$); for volumes larger than the average value $\overline{V}$, $\rho(V)$ follows a power law in the volume ($\rho \sim 1/V^{\alpha}$) that eventually turns into an exponential law ($\rho \sim e^{-\text{const}\cdot V}$) at large enough volumes ($V \gtrsim V_b$). When $\Omega < 1$ the exponential tail starts earlier at $V \simeq V_\epsilon = e^{\pi/(2\sqrt{1-\Omega})}$.

At large volumes, $N \gtrsim \overline{N}$, the probability distribution becomes exponential in N (or, equivalently, power-law in the volume V),

$$\rho(N) \propto e^{-6\Omega N\left(1+\sqrt{1-\frac{1}{\Omega}}\right)} = V^{-2\Omega\left(1+\sqrt{1-\frac{1}{\Omega}}\right)} . \tag{1.9}$$

Then we proceed with the eternal inflation regime. First, we study what happens in the vicinity of the transition point, i.e. when $\Omega = 1 - \epsilon$ with $0 < \epsilon \ll 1$. We find that the probability distribution $\rho(N)$ is not changed until $N \sim \pi/(6\sqrt{\epsilon})$. At large volumes, $N \gtrsim \pi/(6\sqrt{\epsilon})$, it becomes much more strongly suppressed, $\rho(N) \propto e^{-\text{const}\cdot e^{3N}}$. This behavior is easier to interprete in terms of the volume distribution $\rho(V)$ (rather than the e-folding distribution $\rho(N)$). It indicates that if the volume gets large enough, $V \gtrsim e^{\pi/(2\sqrt{\epsilon})}$, the probability for inflation to terminate is exponentially small $P_{\text{ext}} \propto e^{-\text{const}\cdot V}$. Related to that, we find that the total probability for inflation to terminate is of order $e^{-\Omega(3N_c)^2}$ (this also applies for $\epsilon \sim \mathcal{O}(1)$), indicating that it is saturated by the small-N tail of the Gaussian distribution (1.7). This behavior smoothly matches with yet another regime where one can find the probability distribution explicitly—$\Omega \simeq 0$. Here the probability distribution $\rho(V)$ is exponentially small $\rho(V) \propto e^{-V/2}$ for all volumes of interest, $V \gg 1$.

All these considerations were made in the approximation where the inflaton potential goes up to arbitrary high values of the inflaton field. This is clearly unrealistic and we conclude in section 3 by discussing what happens in the presence of a "barrier" at large values of the inflaton field. As expected, the presence of a barrier affects only the far

JHEP04(2009)118

tail of the volume distribution by making it exponentially suppressed at large volumes, $\rho(V) \propto e^{-\text{const}\cdot V}$, for any value of Ω. Note that if the initial value of the inflaton field is not too close to the barrier, this effect is relevant only for inflaton trajectories whose probability is smaller than the uncertainty coming from non-perturbative quantum gravity effects ($\sim e^{-S_{\rm dS}}$). The various behaviors of the probability distribution are summarized in figure 2 that shows the shape of $\rho(V)$ in the different regimes of the volume.

These results imply that the quantum version of the bound (1.1) does hold with $c = 1/2$. In the concluding section 4 we give the physical explanation of the behavior of the probability distribution and show that an inflaton trajectory with more than $S_{\rm dS}/6$ e-foldings and such that inflation terminates globally in the entire space is super-exponentially improbable. We also speculate on the possibility that the value $c = 1/2$ for the coefficient in (1.1) that we obtained in our analysis might have a natural physical interpretation. In the appendix we cross check our results by calculating the average volume directly from the inflaton stochastic equations.

2 From bacteria to inflation

As explained in the introduction, we want to calculate and study the probability distribution $\rho(V, \phi)$ of the reheating volume given a certain initial value of the field ϕ. This calculation does not seem to be straightforward, as the only available definition of the distribution is a rather formal functional integral formula [16]

$$\rho(V,\phi) = \int \mathcal{D}\bar{\phi}\, \mathcal{P}[\bar{\phi},\phi]\, \delta\left[V - \int d^3x\, e^{3Ht_r(\vec{x})}\right] , \tag{2.1}$$

where $\mathcal{D}\bar{\phi}$ is some vaguely defined measure on the set of all possible space-time realizations of the inflaton field, $\mathcal{P}[\bar{\phi},\phi]$ is the probability of a specific realization and $t_r(\vec{x})$ is the reheating time for a given realization as a function of the comoving coordinate $\vec{x}$. Evaluating directly the functional integral is of course a very hard task. As usual with functional integrals, in order to gain more control it is natural to switch to a discretized description of the inflationary dynamics. This approach has been recently developed in [16] and similar models have also been studied in the context of eternal inflation in [33]. Up to small extensions, section 2.1 is mainly a review of the results in [16], which we use to derive the formula for the probability distribution $\rho(V, \phi)$ in section 2.2. The resulting solution for $\rho(V, \phi)$ will be discussed in section 3. As a cross-check of the method, in the appendix we also present a direct computation of the volume average.

2.1 Review of bacteria model

With a biological analogy, consider at $t = 0$ a bacterium that can live in a discrete set of positions along a line (see figure 3). At $t = 1$ the bacterium replicates into N_r copies. Then, each bacterium (independently of all the others) hops with probability p to the neighboring site on its right, and with probability $(1 - p)$ on the left. N_r and p are fixed numbers. At $t = 2$ each second-generation bacterium reproduces itself, and so on. The analogy with the inflationary system is clear: each bacterium represents an Hubble patch; sites are inflaton

JHEP04(2009)118

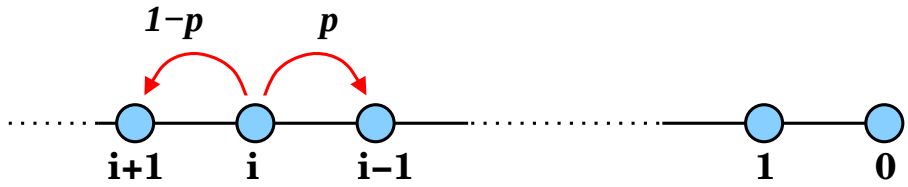

Figure 3. The branching process.

values. Reproduction is the analogue of the Hubble expansion; at every e-folding $\sim e^3$ new Hubble volumes are produced starting from one. From then on the inflaton inside each Hubble volume evolves independently, with a combination of classical rolling and quantum diffusion. This is represented by the random hopping of our bacteria. The difference in the probabilities of moving right and left gives a net drift, and thus corresponds to the classical motion. To complete the analogy we have to assume that there is a "reheating" site, $i = 0$ in the figure: when a bacterium ends up there it stops to reproduce and to move around — it dies. In the bacteriological analogy the reheating volume corresponds to the number of dead bacteria (= non-reproducing Hubble patches) in the asymptotic future. For analogy we denote the latter quantity by V, which of course now takes discrete values. Our task is to study the probability distribution of V as a function of the parameter p. A discrete system like the one we described goes under name of *branching process*, more precisely a multi-type Galton-Watson process (see e.g. ref. [36]).

To connect to the inflationary case, if ϕ is the inflaton, and t is the time of the FRW metric, one can make the following identifications in terms of the position j, time-step n, field-space interval $\Delta\phi$ and time interval Δt,

$$j = \frac{\phi}{\Delta\phi}\,, \qquad n = \frac{t}{\Delta t}\,. \tag{2.2}$$

By taking the continuum limit $\Delta\phi, \Delta t \to 0$ in such a way that

$$\Delta t = \frac{4\pi^2}{H^3}(\Delta\phi)^2\,, \tag{2.3}$$

where H is the Hubble rate in the inflationary process, and by defining N_r as

$$N_r = 1 + 3H\Delta t\,, \tag{2.4}$$

and p by the relationship

$$(1-2p)\frac{\Delta\phi}{\Delta t} = \dot{\phi} \quad \Rightarrow \quad p = \frac{1}{2} + \sqrt{6\pi^2\Omega}\,\frac{\Delta\phi}{H}\,, \tag{2.5}$$

the equation for the probability of a bacterium to be at site j at time n becomes the stochastic equation for the inflaton [10, 11, 34]

$$\frac{4\pi^2}{H^3}\partial_t P(\bar{\phi}, t) = \frac{1}{2}\partial^2_{\bar{\phi}} P(\bar{\phi}, t) + \frac{2\sqrt{6\pi^2\Omega}}{H}\partial_{\bar{\phi}} P(\bar{\phi}, r)\,, \tag{2.6}$$

where $P(\bar{\phi}, t)$ is the probability that the inflaton ϕ after a time t has a value $\bar{\phi}$. In [16] general arguments establishing the matching with the continuum limit were presented and checked in several calculations performed both in terms of the bacteria model and of the inflaton.

Let us therefore study in more detail the bacteria model, and consider a branching process on a line of length L. A convenient tool to study the branching process is the set of generating functions $f_i^{(n)}(s_j)$, where $i, j = 0, \ldots, L$. These are defined as power series

$$f_i^{(n)}(s_j) = \sum_{k_1 \ldots k_L} p^{(n)}_{i;k_0 \ldots k_L} s_0^{k_0} \ldots s_L^{k_L} \,, \tag{2.7}$$

where $p^{(n)}_{i;k_0 \ldots k_L}$ is the probability that, in a branching process that started with a single bacterium at the i-th site after n steps, one has k_0 bacteria at the zeroth site, k_1 bacteria at the first site, etc. It is convenient to combine together all functions $f_i^{(n)}$ with the same number of steps n into a map F_n from the $L+1$-dimensional space of the auxiliary parameters s_i into an $L+1$-dimensional space parameterized by the f_i's. Also in what follows we will sometimes drop the subscript from the s_i variables and denote by s a point in the $L+1$-dimensional space with coordinates $(s_0, \ldots, s_L)$. For example, for a branching process of the sort as described in figure 3, F_1 is given by

$$\begin{aligned} f_0^{(1)}(s_0, \ldots, s_L) &= s_0 \,, \\ f_1^{(1)}(s_0, \ldots, s_L) &= \left((1-p)s_2 + p\, s_0\right)^{N_r} \,, \\ &\vdots \\ f_i^{(1)}(s_0, \ldots, s_L) &= \left((1-p)s_{i+1} + p\, s_{i-1}\right)^{N_r} \,, \\ &\vdots \\ f_L^{(1)}(s_0, \ldots, s_L) &= \left((1-p)s_L + p\, s_{L-1}\right)^{N_r} \,, \end{aligned} \tag{2.8}$$

where we have made a specific choice of boundary conditions at the site L, which we will refer to as the "barrier". The particular choice of the boundary condition will affect only very marginally our results. The main property making generating functions useful is the iterative relation

$$F_{n+1} = F_1(F_n) \,. \tag{2.9}$$

This property is straightforward to check by making use of the definition of the branching process and elementary properties of probabilities.

We will be interested in the late time behavior of the branching process, which is determined by the asymptotic function F_∞. The iterative property (2.9) implies that

$$F_1(F_\infty) = F_\infty \,, \tag{2.10}$$

i.e. the set of values of the function F_∞ is a subset of the fixed points of the function F_1, such that

$$F_1(s) = s \,. \tag{2.11}$$

JHEP04(2009)118

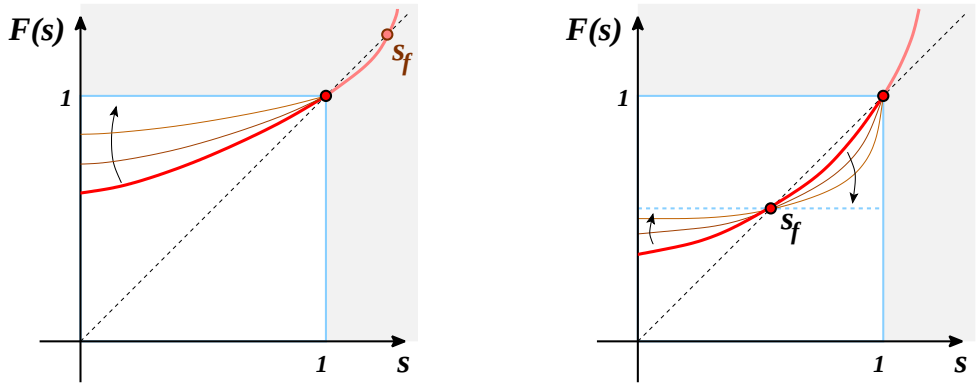

Figure 4. *Left:* Plot of $F_1(s)$ restricted to the hypercube I_L and with $s_0 = 1$, for large p *(thick curve)*. The only fixed point in the unit cube is $s = 1$. Further applications of F_1 *(thinner curves)* drive the curve to the $F_\infty = 1$ line. right: For smaller p's a new fixed point s_f enters the unit cube. Now the limiting line is $F_\infty = s_f$.

For our purposes it is enough to study the mapping F_1 inside the $L+1$-dimensional cube I_{L+1} of unit size, $0 \leq s_i < 1$. The definition (2.7) of the generating functions implies that all partial derivatives of $F_1(s)$ are positive. Also, the normalization of probabilities implies that

$$F_1(1, \ldots, 1) = (1, \ldots, 1) \equiv \vec{1}\,.$$

In the bacteria model, it is rather straightforward to see how the transition to the eternal inflationary regime happens. For this, it is useful to restrict the function F to the L-dimensional hypercube I_L with $s_0 = 1$, which amounts to marginalizing over the number of dead bacteria (see eq. (2.7)). Note that, if the mapping F_1 has no other fixed points in the cube I_L apart from $\vec{1}$ (see figure 4), then

$$F_\infty|_{s_0=1} = \vec{1}\,.$$

By definition of the generating functions, eq. (2.7), this means that in the late time asymptotics with probability one there are no alive bacteria at any of the sites. The extinction probability is exactly equal to one (inflation ends). The situation changes when a non-trivial fixed point s_f solving eq. (2.11) enters the region I_L (see figure 4). Now one has

$$F_\infty|_{s_0=1} = (1, s_f) < \vec{1}\,. \tag{2.12}$$

This implies that, as before, the probability to have any finite non-zero number of alive bacteria at any site vanishes. However, the probabilities to have zero bacteria at the various sites,

$$p^{(\infty)}_{i;\text{any},0\ldots0} = f_i^{(\infty)}(0) = (s_f)_i\,, \qquad i \neq 0\,, \tag{2.13}$$

are all less than one. This means that there is a non-vanishing probability that the population never dies out and that the total number of bacteria grows indefinitely at late times. This corresponds to the eternal inflation regime. Clearly, this implies that the number of

JHEP04(2009)118

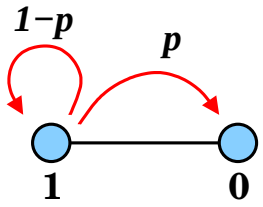

Figure 5. The 2-site branching process.

dead bacteria also has a finite probability to grow indefinitely; in the context of eternal inflation this translates into

$$\int_0^\infty dV\,\rho(V,\phi) < 1\,.$$

In the continuum limit and with infinite barrier this transition happens at $\Omega = 1$.

We would like to stress that F_∞ is a function of s_0 only. Mathematically this follows from the convexity of F_1 with respect to s_i, $i \neq 0$, from the fact that F_1 is defined between 0 and 1, and that $F_1(\vec{1}) = \vec{1}$ (see figure 4). This can also be intuitively understood in the following way: in the non-eternal regime, in the infinite future there is zero probability of having any bacteria alive, so F_∞ can not depend on any of the s_i, $i \neq 0$. In the eternal inflation case, the population either extinguishes or becomes infinite. In either case, the probability of finding a finite number of bacteria at any site is zero, which again forbids any dependence on s_i, $i \neq 0$. Therefore, $F_\infty = F_\infty(s_0)$. Eq. (2.10) for the fixed point then becomes

$$\begin{aligned}
f_0^{(\infty)}(s_0) &= s_0\,,\\
&\vdots\\
f_i^{(\infty)}(s_0) &= \Big((1-p) f_{i+1}^{(\infty)}(s_0) + p\, f_{i-1}^{(\infty)}(s_0)\Big)^{N_r}\,,\\
&\vdots\\
f_L^{(\infty)}(s_0) &= \Big((1-p) f_L^{(\infty)}(s_0) + p\, f_{L-1}^{(\infty)}(s_0)\Big)^{N_r}\,.
\end{aligned} \tag{2.14}$$

This is the set of equations that determine $f_i^{(\infty)}(s_0)$. Once $f_i^{(\infty)}(s_0)$ is found, one can extract the asymptotic probability distribution $p_{i;k_0}^{(\infty)}$ using eq. (2.7).

2.1.1 An example: the 2-sites case

We find it instructive to illustrate the general formalism using a simple explicit example. Consider the minimal branching process with just two sites and $N_r = 2$ copies at each reproduction event (see figure 5). In this case the generating functions (2.7) are particularly simple,

$$\begin{aligned}
f_0^{(1)}(s_0,s_1) &= s_0\,,\\
f_1^{(1)}(s_0,s_1) &= \big((1-p)s_1 + p s_0\big)^2\,.
\end{aligned} \tag{2.15}$$

It is straightforward to apply here the generic results discussed in the last section. $f_i^{(\infty)}(s_0)$ is given by the fixed point of the mapping defined in eq. (2.15) inside the unit interval $0 \leq s_i \leq 1$. We obtain

$$f_0^{(\infty)}(s_0) = s_0\,, \tag{2.16}$$

$$f_1^{(\infty)}(s_0) = \frac{1 - 2ps_0 + 2p^2 s_0 - \sqrt{1 - 4p(1-p)s_0}}{2(1-p)^2}\,. \tag{2.17}$$

The extinction probability is given by

$$P_{\rm ext} = \sum_{k=0}^{\infty} p_k = f_1^{(\infty)}(1) = \frac{1 - 2p + 2p^2 - \sqrt{(1-2p)^2}}{2(1-p)^2} = \begin{cases} 1 & p > 1/2 \\ \left(\frac{p}{1-p}\right)^2 & p < 1/2 \end{cases}\,, \tag{2.18}$$

where $p_k \equiv p_{1;k\,0}^{(\infty)}$. The extinction probability indeed drops below one for $p < 1/2$. We get the quite intuitive result that the critical probability is $p_c = 1/2$. By Taylor expanding $f_i^{(\infty)}(s_0)$, we can obtain the probability of the volume p_k as in eq. (2.7)

$$f_1^{(\infty)}(s_0) = \frac{1}{2(1-p)^2} \sum_{k=2}^{\infty} \frac{(2k-3)!}{2^{2k-2} k!(k-2)!} (4p(1-p)s_0)^k\,, \tag{2.19}$$

which allows us to extract the large-k asymptotic of the probability distribution p_k,

$$p_k \sim \frac{1}{(1-p)^2} \; \frac{1}{k^{3/2}} e^{-k \log\left(\frac{1}{4p(1-p)}\right)}\,. \tag{2.20}$$

We see that the probability for large volumes goes to zero exponentially fast for any $p \neq p_c = 1/2$ (notice that $4p(1-p) \leq 1$ for any p, and becomes equal to one only for $p = 1/2$). At $p = p_c$ the exponential suppression disappears and we are left with a power law behavior, corresponding to the singularity of $f_1^{(\infty)}(s_0)$ at $s_0 = 1$, as a result the probability distribution becomes not normalized for $p \leq p_c$. This can be understood in the following way. So far we have studied the probability distribution in the infinite time limit. If instead we let the process go on only for a finite number of time steps n, the probability distribution develops a bump at large volume (see [16] for details), which can be roughly thought of as a piece proportional to $\Theta(1 - P_{\rm ext})\delta(k - 2^n)$. For $p \leq p_c$, in the limit $n \to \infty$, the $\delta-$function migrates to infinity and makes all the moments of the volume diverge. In our calculation, we can not see such a δ-function because we have already taken the limit of infinite time steps, but still we are left with a non-normalized distribution. Because of this even for $p < p_c$ all the moments of the volume diverge even if the probability distribution goes exponentially fast to zero at infinity,.

2.2 The equation for $\rho(V)$

We want now to take the continuum limit of the bacteria model as explained in the beginning of section 2.1. According to eq. (2.2), we define $f^{(\infty)}(\phi; s_0) = f_{\phi/\Delta\phi}^{(\infty)}(s_0)$ so that the

system in eq. (2.14) now becomes

$$\begin{aligned} f^{(\infty)}(0,s_0) &= s_0\,, \\ &\vdots \\ f^{(\infty)}(\phi;s_0) &= \Big((1-p)f^{(\infty)}(\phi+\Delta\phi;s_0)+p\,f^{(\infty)}(\phi-\Delta\phi;s_0)\Big)^{N_r}\,, \\ &\vdots \\ f^{(\infty)}(\phi_b;s_0) &= \Big((1-p)f^{(\infty)}(\phi_b;s_0)+p\,f^{(\infty)}(\phi_b-\Delta\phi;s_0)\Big)^{N_r}\,, \end{aligned} \tag{2.21}$$

where ϕ_b represents the value of ϕ at the barrier.

By taking the limit $\Delta\phi \to 0$ $\Delta t \to 0$ according to the prescription given in eqs. (2.3), (2.4), and (2.5) we obtain the following second order differential equation

$$\frac{1}{2}\frac{\partial^2}{\partial\phi^2}f^{(\infty)}(\phi;s_0) - \frac{2\pi\sqrt{6\Omega}}{H}\frac{\partial}{\partial\phi}f^{(\infty)}(\phi;s_0) + \frac{12\pi^2}{H^2}f^{(\infty)}(\phi;s_0)\log\Big[f^{(\infty)}(\phi;s_0)\Big] = 0\,, \tag{2.22}$$

with the following two boundary conditions

$$\begin{aligned} f^{(\infty)}(0;s_0) &= s_0\,, \\ \frac{\partial}{\partial\phi}f^{(\infty)}(\phi;s_0)\Big|_{\phi_b} &= 0\,. \end{aligned} \tag{2.23}$$

in agreement with [32, 35] where the same equation has been obtained in a different way. The second derivative term in eq. (2.22) comes from the quantum fluctuations of the inflaton (equivalent to the random jumps of the bacteria), the first derivative term comes from the classical drift (in fact it is proportional to Ω), and the log in the last term comes from the production of independent Hubble patches (equivalent to the reproduction of bacteria).

This equation will be central in the rest of paper: $f(\phi;s_0)$ is the Laplace transform of the probability of obtaining a certain reheating volume starting from any initial value of ϕ. Indeed, in the discrete model, from the definition in eq. (2.7), the generating function at infinite time is connected to the probability $p_{j,k}$ of having k dead bacteria at infinite time starting with one bacterium at the site j by

$$f_j^{(\infty)}(s_0) = \sum_{k=0}^{\infty} p_{j,k}\, s_0^k\,. \tag{2.24}$$

Taking the continuum limit we get

$$f^{(\infty)}(\phi;s_0) = \int_0^{\infty} dV\,\rho(\phi,V)\,s_0^V\,. \tag{2.25}$$

This expression can be inverted to obtain the probability distribution for the volume

$$\rho(\phi,V) = \frac{1}{2\pi i}\int_{\gamma-i\infty}^{\gamma+i\infty} d\left(-\log(s_0)\right) f^{(\infty)}(\phi;s_0)e^{-V\log(s_0)} \tag{2.26}$$

JHEP04(2009)118

where γ must be chosen such that $\mathrm{Re}(\gamma) > -\log(s_0^{\mathrm{sing}})$ for any singularity s_0^{sing} of $f(\phi; s_0)$.[3] Notice that in eq. (2.26) we need to analytically continue the function $f^{(\infty)}(\phi; s_0)$ to unphysical values of s_0 ($s_0 \notin [0,1]$), which actually dominate the integral at large volumes as we will see in section 3. We have therefore obtained a procedure to compute the probability distribution of the reheating volume: solve the differential equation (2.22), and then perform the anti-Laplace transform (2.26).

3 Probability distribution of the volume after inflation

In the previous section we saw that the probability distribution of the volume can be calculated in two steps. The first is to solve the differential equation (2.22). For convenience we rewrite it here as

$$\ddot{f}(\tau; z) - 2\sqrt{\Omega}\dot{f}(\tau; z) + f(\tau; z)\log[f(\tau; z)] = 0\,, \tag{3.1}$$

where the dot represents a partial derivative with respect to τ and $f(\tau; z)$, τ and z are related to $f^{(\infty)}(\phi; s_0)$, ϕ and s_0 of the previous section via

$$f(\tau; z) \equiv f^{(\infty)}(\phi; s_0)\,, \tag{3.2}$$

$$\tau \equiv 2\pi\sqrt{6}\frac{\phi}{H} = 6\sqrt{\Omega}N_c\,, \tag{3.3}$$

$$z \equiv -\log(s_0)\,, \tag{3.4}$$

with N_c being the classical number of e-foldings ($N_c \equiv -H\phi/\dot{\phi}$). The solution $f(\tau, z)$ has also to satisfy the following boundary conditions

$$f(0; z) = s_0 = e^{-z}\,, \tag{3.5}$$

$$\dot{f}(\tau_b; z) = 0\,, \tag{3.6}$$

and the constraint

$$f(\tau; z) \in [0, 1]\,. \tag{3.7}$$

The second step is to calculate the integral

$$\rho(V, \tau) = \frac{1}{2\pi i}\int_{0^+-i\infty}^{0^++i\infty} dz\, f(\tau; z)e^{zV}\,, \tag{3.8}$$

that gives the probability distribution $\rho(V, \tau)$ to find a volume V at the end of an inflationary phase that started with the inflaton at the position $\phi = H\tau/(2\pi\sqrt{6})$. Recall that the volume V that enters in eq. (3.8) is dimensionless because it has been rescaled by the initial volume V_0 before inflation, i.e. $V = \mathrm{Vol}/V_0$, with Vol being the physical volume. Notice that some properties of $\rho(V)$ can be obtained without evaluating the integral (3.8),

[3] From eq. (2.25) we see that $f^{(\infty)}(\phi; s_0)$ cannot have singularities for $\mathrm{Re}(\log(s_0)) < 0$, therefore eq. (2.26) holds for every $\gamma > 0$.

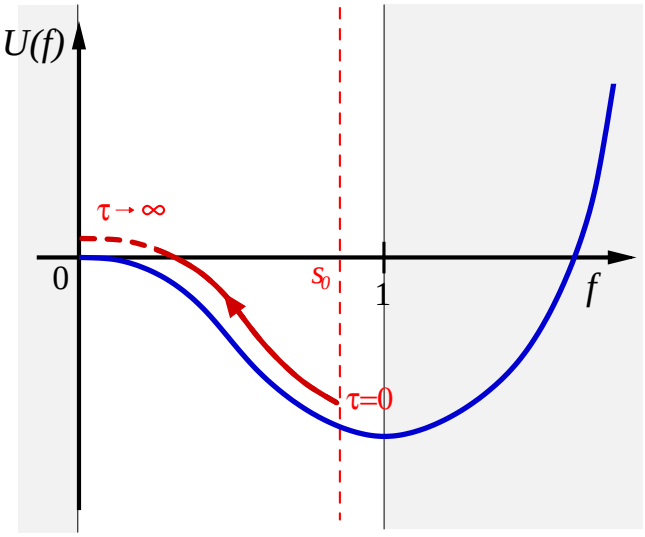

Figure 6. The potential U(f) of eq. (3.11). In the limit $\tau_b \to \infty$, the solution of the mechanical problem (3.1) represents the motion of a particle starting at $\tau = 0$ in $f = s_0$, rolling uphill with an anti-friction term and stopping on the top $f = 0$ in an infinite time.

but just by studying the solution $f(\tau; z)$ around the point $z = 0$. Indeed the momenta of the distribution are simply related to the Taylor coefficients of $f(\tau; z)$ around $z = 0$ since

$$\langle V^n \rangle = \int_0^\infty dV\, V^n \rho(V, \tau) = (-1)^n \left. \frac{\partial^n f(\tau; z)}{\partial z^n} \right|_{z=0} . \tag{3.9}$$

It follows that the total probability to exit inflation globally is just fixed by $f(\tau; 0)$,

$$P_{\rm ext} \equiv \int_0^\infty dV \rho(V, \tau) = f(\tau; 0) . \tag{3.10}$$

We proceed now with the study of the solutions of eq. (3.1). This equation describes the motion of the particle in a potential

$$\mathrm{U}(f) = \frac{f^2}{4} \left(\log f^2 - 1 \right) , \tag{3.11}$$

with an anti-friction term (see figure 6). Unfortunately an explicit solution to eq. (3.1) is not known. However we will still be able to recover many properties of $\rho(V, \tau)$ by analyzing the analytic structure of the solution and by studying the problem in different limits. The boundary conditions (3.5) and (3.6) as well as the condition $f \in [0, 1]$ constrain the solution to start from the point $f = s_0$ at $\tau = 0$ and to travel up-hill up to some point $f_* \in (0, s_0)$ where the velocity reaches zero at time τ_b. We will focus on the case where $\tau_b \to +\infty$, and come back to the case of finite τ_b at the end of this section. In the $\tau_b \to +\infty$ case, the solution has to reach zero velocity only after an infinite time, and in doing so, it has to stay always within the interval $f \in [0, 1]$. The only way to achieve this is for the solution to reach the top of the hill $f = 0$ in infinite time.

JHEP04(2009)118

Let us see that such a solution exists for any $s_0 < 1$. Clearly for large enough initial velocities the solution overshoots the maximum and goes to the $f < 0$ region, while for small enough velocities, the solution does not reach the top. Therefore, there is a critical initial velocity separating these two regimes such that the solution stops at $f = 0$ in an infinite time. This can also be explicitly verified by finding, as we will show later, an asymptotic form of this solution in the region $0 < f \ll 1$,

$$f \sim e^{-\frac{1}{4}(\tau+\tau_0)^2}\,, \tag{3.12}$$

where τ_0 is an integration constant.

The case $s_0 = 1$ is different. For a solution that starts at $f = 1$ at early times we can approximate the potential $\mathrm{U}(f)$ with an harmonic oscillator to obtain

$$\ddot{f} - 2\sqrt{\Omega}\dot{f} + f - 1 = 0\,, \tag{3.13}$$

whose general solution is of the form

$$f = 1 - e^{\sqrt{\Omega}\tau}\left(Ae^{\sqrt{\Omega-1}\tau} + Be^{-\sqrt{\Omega-1}\tau}\right)\,. \tag{3.14}$$

This shows that for $\Omega > 1$ the solution is 'over-anti-dumped' and does not have a turning point, while for $\Omega < 1$ the solution can oscillate. This behavior persists at the non-linear level as well — it is straightforward to check that the turning force due to the potential (3.11) is always smaller than the turning force due to the harmonic potential in (3.13), so that no turning point exists for $\Omega > 1$ for the non-linear mechanical problem (3.1) as well. Consequently, at $s_0 = 1$ the solution that stops on the top of the hill exists only at $\Omega < 1$. This solution describes a non-trivial fixed point (2.12). Its presence indicates that inflation is eternal at $\Omega < 1$. Instead, at $\Omega > 1$ the solution that reaches the top of the hill in an infinite time $\tau \to +\infty$ starts at $f = 1$ in the infinite past, $\tau = -\infty$; while all solutions that start at $f = 1$ at finite time overshoot the top of the hill.

We illustrate the behavior of the solutions in the two different regimes in figure 7. This plot makes very explicit the transition to the eternal regime at $\Omega = 1$. At $\Omega > 1$ by taking the limit $s_0 \to 1$ one gets $f(\tau; 0) = 1$ for every τ so that the extinction probability is $P_{\rm ext} = 1$. On the other hand, in the same limit at $\Omega < 1$ one obtains a non-trivial function $f(\tau; 0)$ that leaves the origin in a time of order $1/\sqrt{1-\Omega}$, therefore there is a non-vanishing probability to inflate forever, $P_{\rm ext} = 1 - f(\tau; 0)$.

In the following subsections we will present estimates for $\rho(V, \tau)$ in different regimes and discuss finite-barrier effects. However, before entering the analysis of the probability distribution itself, we would like to discuss first its moments, which can be derived exactly in a straightforward way from the master differential equation (3.1).

3.1 Moments of the probability distribution and critical points

In spite of the fact that the phase transition happens at the critical value $\Omega = 1$, in [16] it was shown that, in the infinite barrier limit, the moments of the probability distribution start diverging at different values of Ω: the higher the moment, the higher the value of Ω at which they diverge. On the other hand, in the finite barrier case all the moments diverge

JHEP04(2009)118

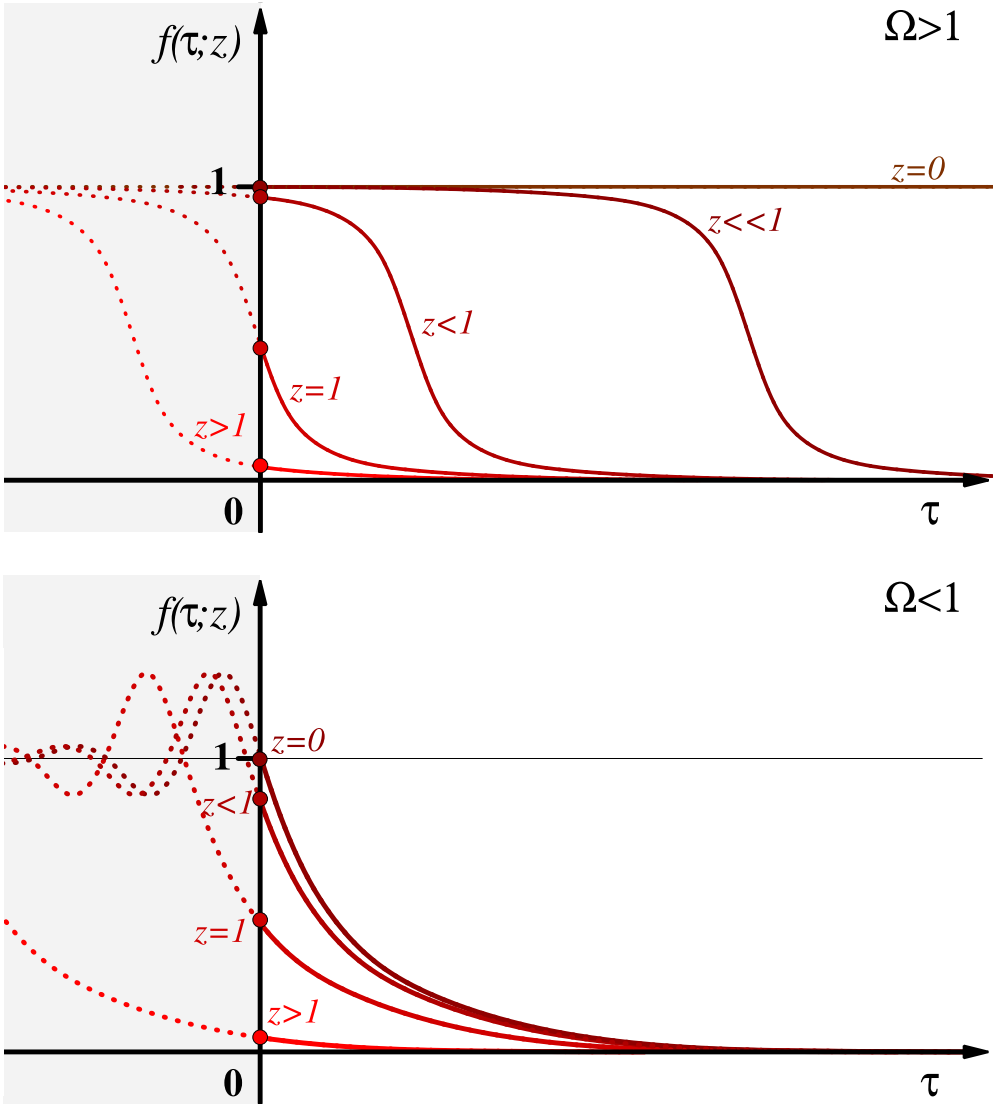

Figure 7. Schematic plots of the solutions $f(\tau; z)$ as a function of τ for different choices of the boundary condition z and for $\Omega > 1$ (top) and $\Omega < 1$ (bottom). For $\Omega > 1$ when $z \to 0$ the solution approaches $f(\tau; 0) = 1$ for every finite τ's — the probability to end inflation globally is 1; for $\Omega < 1$ in the same limit the solution approaches a non-trivial function with $f(\tau; 0) \ll 1$ for large τ—the probability to end inflation globally is small.

at the critical value $\Omega = 1$. In the first part of this section, we will rederive these results in a rather quick and different way, obtaining also the general formula for the critical value Ω at which each moment diverge. Then, in the second part, we will describe a procedure derived from the master differential equation (3.1) that allows us to easily compute the explicit value of each moment as a function of Ω.

As shown in the previous section from eq. (3.9), it is possible to extract the moments of the probability distribution $\rho(V, \tau)$ directly from $f(\tau; z)$ without the need of performing

JHEP04(2009)118

explicitly the anti-Laplace transform. The n-th moment is indeed proportional to the n-th derivative of $f(\tau; z)$ with respect to z, at $z = 0$. Divergences in the moments thus correspond to a non-analyticity of $f(\tau; z)$ at $z = 0$. Therefore it is enough to study the solution of the differential equation near the point $z = 0$. Notice that, before entering the eternal regime, at $\Omega > 1$, for every finite fixed value of τ and for smaller and smaller values of z, the solution is better and better described by the linear approximation of eq. (3.14) (see figure 7), which we conveniently rewrite here as

$$f_{\rm lin}(\tau; z) = 1 - e^{\omega_-(\tau+\tau_0)} - \sigma e^{\omega_+(\tau+\tau_0)}\,, \tag{3.15}$$

where

$$\omega_\pm \equiv \sqrt{\Omega} \pm \sqrt{\Omega - 1}$$

and σ and τ_0 are the two constant of integration. In the infinite barrier case the boundary condition (3.6) corresponds to requiring that the solution stops on top of the hill ($f = 0$) in an infinite time. Notice that since both this boundary condition and the differential equation are invariant under shifts of τ we are left with a one-parameter family of solutions that are related by a shift in τ, i.e. the parameter τ_0. The latter is fixed by imposing the boundary condition (3.5), namely

$$f_{\rm lin}(0; z) = 1 - e^{\omega_-\tau_0} - \sigma e^{\omega_+\tau_0} = e^{-z}\,. \tag{3.16}$$

This means that all the dependence on z is in the parameter τ_0, while σ is fixed by the boundary condition at infinity and is independent of z. Using eq. (3.16) the solution can be rewritten as

$$\begin{aligned} f_{\rm lin}(\tau; z) &= 1 - \left(1 - e^{-z}\right) e^{\omega_-\tau} - \sigma e^{\omega_+\tau_0}\left(e^{\omega_+\tau} - e^{\omega_-\tau}\right) \\ &\simeq 1 - z e^{\omega_-\tau} - \sigma z^{\omega_+^2} e^{\omega_+\tau}\,, \end{aligned} \tag{3.17}$$

where in the second line we have used the approximate solution $\tau_0 \approx \log(z)/\omega_-$ from eq. (3.16) and dropped a subleading exponent in the last term.

Notice also that the last term, in general, is not analytic in $z = 0$. Indeed if we calculate the n-th derivative of $f_{\rm lin}(\tau; z)$ with respect to z we get

$$f^{(n)}_{\rm lin}(\tau; z) \sim z^{\omega_+^2 - n} e^{\omega_+\tau} \tag{3.18}$$

so that the moment $\langle V^n \rangle$ starts diverging when ω_+^2 becomes smaller than n, i.e. at

$$\Omega = \frac{(n+1)^2}{4n}\,. \tag{3.19}$$

For instance, in the case of the variance ($n = 2$), we get $\Omega = 9/8$ as critical value, in perfect agreement with the lengthy calculation of [16] that used directly the inflaton stochastic equations. In the presence of a finite barrier this argument breaks down because now also σ depends on z and the analytic structure around the origin changes. In fact, for small enough values of z, $f(\tau; z)$ is still well described by the linear approximation around $f = 1$

JHEP04(2009)118

even at the barrier τ_b. It is not difficult then to solve the differential equation in the linearized limit with a finite barrier. What we get in this case is

$$f_{\rm lin}(\tau;z) = 1-(1-e^{-z})\frac{e^{\omega_+\tau+\omega_-\tau_b}-\omega_+^2 e^{\omega_-\tau+\omega_+\tau_b}}{e^{\omega_-\tau_b}-\omega_+^2 e^{\omega_+\tau_b}}\,, \tag{3.20}$$

which is analytic in $z=0$ for all values of Ω, implying that all the moments converge for $\Omega > 1$. Although we expect the linearized approximation to work better and better as $z \to 0$, we cannot be sure yet whether non-analytic terms may arise from subleading non-linear corrections. Still this argument suggests that the finite barrier case behaves differently than the infinite barrier case.

As a proof of this statement we will now present a method to derive exactly all the moments. Indeed, even though we are not able to solve analytically the non-linear differential equation (3.1), the equations for the moments are linear and can be solved explicitly. They can be obtained by simply deriving n times the eq. (3.1) with respect to z at $z=0$. For example by deriving (3.1) once with respect to z we get

$$\ddot{f}' - 2\sqrt{\Omega}\dot{f}' + f' + f'\log f = 0\,, \tag{3.21}$$

where "dots" represent derivatives with respect to τ and " $'$ " with respect to z. Since for $z=0$ $f=1$ we get a linear differential equation for $f_0' \equiv f'(\tau;0) = -\langle V\rangle$ with solution

$$f_0' = Ae^{\omega_+\tau} + Be^{\omega_-\tau}\,. \tag{3.22}$$

The constants of integration A and B can be fixed using the derivative of the boundary conditions (3.5) and (3.6), namely

$$f_0'(0) = -1\,, \qquad \dot{f}_0'(\tau_b) = 0\,. \tag{3.23}$$

This way we get

$$\langle V\rangle = -f_0'(\tau) = \frac{e^{\omega_+\tau+\omega_-\tau_b}-\omega_+^2 e^{\omega_-\tau+\omega_+\tau_b}}{e^{\omega_-\tau_b}-\omega_+^2 e^{\omega_+\tau_b}}\,, \tag{3.24}$$

which in the large τ_b limit gives (see figure 8)

$$\lim_{\tau_b\to\infty}\langle V\rangle = e^{\omega_-\tau} = e^{3N_c\frac{2}{1+\sqrt{1-1/\Omega}}}\,. \tag{3.25}$$

This results nicely agrees with the explicit calculation from the inflaton equation (see the appendix) and with the result from the probability distribution $\rho(V,\tau)$ that we will derive in the next sections. Notice that for large Ω one recovers the classical limit for the average volume $V_c = e^{3N_c}$. With very little effort eq. (3.1) gave us the formula for the average volume in both finite and infinite barrier cases.

Roughly with the same amount of work we can obtain also the expression for any higher moment. By deriving eq. (3.21) with respect to z a second time we obtain

$$\ddot{f}'' - 2\sqrt{\Omega}\dot{f}'' + f'' + f''\log f + \frac{f'^2}{f} = 0\,, \tag{3.26}$$

JHEP04(2009)118

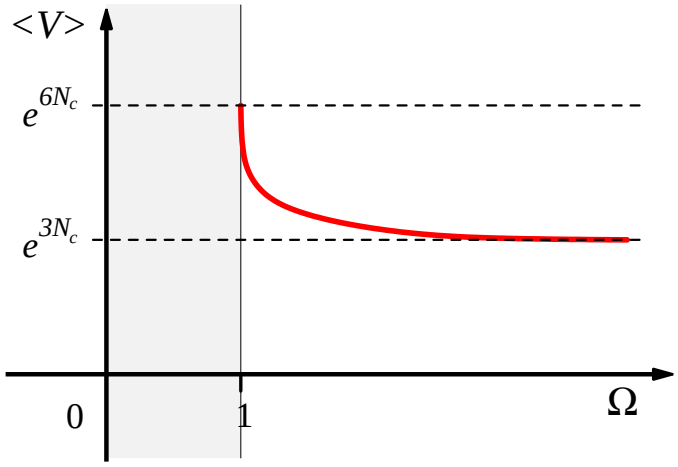

Figure 8. Average volume as a function of Ω, with $N_c \equiv \frac{2\pi^2}{\Omega}\frac{\phi}{H} = \frac{\tau}{6\sqrt{\Omega}}$.

which again gives a linear differential equation at $z = 0$,

$$\ddot{f}_0'' - 2\sqrt{\Omega}\dot{f}_0'' + f_0'' = -f_0'^2\,, \tag{3.27}$$

this time with a non-homogeneous source term. The latter however is an exponential, therefore the differential equation can be easily solved analytically. Imposing the boundary conditions

$$f_0''(0) = 1\,, \qquad \dot{f}_0''(\tau_b) = 0\,, \tag{3.28}$$

the result for the second moment is

$$\begin{aligned}\langle V^2\rangle = f_0''(\tau) = {} & \frac{\omega_+^6 e^{\frac{2\tau}{\omega_+}+2\tau_b\omega_+}}{\left(\omega_+^2-2\right)\left(e^{\tau_b/\omega_+}-e^{\tau_b\omega_+}\omega_+^2\right)^2} - \frac{2\omega_+^4 e^{2\tau_b\omega_+}\left(e^{\frac{\tau_b}{\omega_+}+\tau\omega_+}-e^{\frac{\tau}{\omega_+}+\tau_b\omega_+}\omega_+^2\right)}{\left(\omega_+^2-2\right)\left(e^{\tau_b/\omega_+}-e^{\tau_b\omega_+}\omega_+^2\right)^3} \\ & - \frac{4\omega_+^2 e^{\omega_+\tau_b+\frac{\tau_b}{\omega_+}}\left(e^{\frac{\tau_b}{\omega_+}+\tau\omega_+}-e^{\frac{\tau}{\omega_+}+\tau_b\omega_+}\omega_+^2\right)}{\left(e^{\tau_b/\omega_+}-e^{\tau_b\omega_+}\omega_+^2\right)^3} + \frac{2\omega_+^2 e^{\frac{2\tau_b}{\omega_+}}\left(e^{\frac{\tau_b}{\omega_+}+\tau\omega_+}-e^{\frac{\tau}{\omega_+}+\tau_b\omega_+}\omega_+^2\right)}{\left(2\omega_+^2-1\right)\left(e^{\tau_b/\omega_+}-e^{\tau_b\omega_+}\omega_+^2\right)^3} \\ & + \frac{8\omega_+^2 e^{2\omega_+\tau_b+\frac{2\tau_b}{\omega_+}}\left(e^{\tau\omega_+}-e^{\tau/\omega_+}\right)\left(\omega_+^2-1\right)^2\left(\omega_+^2+1\right)}{\left(e^{\tau_b/\omega_+}-e^{\tau_b\omega_+}\omega_+^2\right)^3\left(2\omega_+^4-5\omega_+^2+2\right)} + \frac{2\omega_+^2 e^{\omega_+\tau+\frac{\tau}{\omega_+}+\tau_b\omega_++\frac{\tau_b}{\omega_+}}}{\left(e^{\tau_b/\omega_+}-e^{\tau_b\omega_+}\omega_+^2\right)^2} \\ & - \frac{e^{\frac{2\tau_b}{\omega_+}+2\tau\omega_+}}{\left(2\omega_+^2-1\right)\left(e^{\tau_b/\omega_+}-e^{\tau_b\omega_+}\omega_+^2\right)^2}\,,\end{aligned} \tag{3.29}$$

where the length of the expression indicates how non-trivial it would have been to obtain this result directly from the inflaton equation. In the large barrier limit the asymptotic form of eq. (3.29) for $\Omega > 1$ reads

$$\langle V^2\rangle \overset{\tau_b\gg 1}{\longrightarrow} \frac{\omega_+^2}{\omega_+^2-2}\left(1-2\frac{e^{-\omega_-\tau}}{\omega_+^2}\right)e^{2\omega_-\tau} + \frac{8(\omega_+^2-1)^2(\omega_+^2+1)}{\omega_+^4(2\omega_+-1)(2-\omega_+^2)}e^{-(\omega_+^2-2)\omega_-\tau_b+\omega_+\tau}\,, \tag{3.30}$$

JHEP04(2009)118

the divergence at $\omega_+^2 = 2$ (i.e. $\Omega = 9/8$) is manifest, in particular the last term vanishes for $\omega_+^2 > 2$ in the limit $\tau_b \to \infty$, while it explodes for $\omega_+^2 \leq 2$. It is less manifest from eq. (3.29) the fact that, with a finite barrier, there is no divergence; for this propose we give here the expression for eq. (3.29) at $\Omega = 9/8$

$$\langle V^2 \rangle\big|_{\Omega=9/8} = \sqrt{2}\tau_b(1 - e^{-\tau/\sqrt{2}})e^{\sqrt{2}\tau} + \dots\,, \tag{3.31}$$

which shows that, up to sub-dominant terms in the large barrier limit (the dots), the result is finite but linear in τ_b, explaining the divergence in the infinite barrier case.

We could keep going calculating higher moments, indeed for the n-th moment we have just to solve the following linear differential equation

$$\ddot{f}_0^{(n)} - 2\sqrt{\Omega}\dot{f}_0^{(n)} + f_0^{(n)} = J^{(n)}\,, \tag{3.32}$$

$$f_0^{(n)}(0) = (-1)^n\,, \tag{3.33}$$

$$\dot{f}_0^{(n)}(\tau_b) = 0\,, \tag{3.34}$$

where the source $J^{(n)}$ is a polynomium of degree n of the lower moments ($f_0^{(k)}$ with $k < n$)

$$J^{(n)} = \partial_z^n [f(\log f - 1)]\big|_{z=0}\,, \tag{3.35}$$

which will then be a sum of exponentials of the form $e^{k\omega_\pm \tau}$ at most of degree $k = n$.

Iterating the analysis it is possible to check that, in the infinite barrier limit, the critical value of Ω where the n-th moment diverges perfectly agrees with eq. (3.19), while for finite barriers the moments converge for every $\Omega > 1$.

3.2 $\Omega \gg 1$: classical limit

Let us now find approximations for the probability distribution $\rho(V)$ in different regimes by directly using the Laplace transform formula (3.8). The first case we will study is the limit $\Omega \gg 1$, which corresponds to the conventional slow-roll inflation, far from the eternal regime. As expected, we will see explicitly that in this case the volume probability is sharply peaked around the volume corresponding to the classical inflaton trajectory. The main reason to start with this case is that we will be able to find an explicit solution to the mechanical problem (3.1). This will help us to develop an intuition on how to proceed also for generic values of Ω, where such a solution is absent.

To analyze the large Ω limit it is convenient to rescale the time variable τ as

$$\tau = 2\sqrt{\Omega}\tilde{\tau}\,. \tag{3.36}$$

The new time variable $\tilde{\tau}$ measures the number of classical e-foldings N_c,

$$\tilde{\tau} = 3N_c\,. \tag{3.37}$$

Then the mechanical equation (3.1) takes the following form

$$\frac{1}{4\Omega}\frac{\partial^2 f}{\partial \tilde{\tau}^2} - \frac{\partial f}{\partial \tilde{\tau}} + f\log f = 0\,. \tag{3.38}$$

JHEP04(2009)118

It is useful to present f in the exponential form

$$f = e^{-g}\,, \tag{3.39}$$

then the function g satisfies

$$\frac{1}{4\Omega}\left[\frac{\partial^2 g}{\partial\tilde{\tau}^2} - \left(\frac{\partial g}{\partial\tilde{\tau}}\right)^2\right] - \frac{\partial g}{\partial\tilde{\tau}} + g = 0\,. \tag{3.40}$$

The most straightforward way to do the large Ω expansion would be, as a zeroth order approximation, to drop the first two terms in this equation. This would give

$$g = e^{\tilde{\tau}+\tilde{\tau}_0}\,, \tag{3.41}$$

where $\tilde{\tau}_0$ is an integration constant. This translates into

$$f = e^{-z\,e^{\tilde{\tau}}}\,, \tag{3.42}$$

when we fix $\tilde{\tau}_0$ to match the boundary conditions for f. The corresponding probability distribution that we obtain from eq. (3.8) is

$$\rho(V,\tau) = \delta(V - e^{3N_c})\,, \tag{3.43}$$

i.e. the inflaton follows the classical trajectory, exactly what expected in the classical limit where quantum fluctuations can be neglected. However, there is a problem to use this solution as a basis for a systematic expansion around $1/\Omega = 0$ because the corrections due to the dropped terms in (3.40) are not always small. Indeed, for $\tilde{\tau} \gg \log\Omega$ one has $\dot{g}^2/\Omega \gg g, \dot{g}$ in this case. We can get around this problem by keeping this dangerous term in (3.40), and dropping only the very first one (similarly to the WKB approximation). Now we have the following equation

$$\frac{1}{4\Omega}\left(\frac{\partial g}{\partial\tilde{\tau}}\right)^2 + \frac{\partial g}{\partial\tilde{\tau}} - g = 0 \tag{3.44}$$

that after integration gives g as a solution of the following algebraic equation,

$$Ge^G = e^{\tilde{\tau}+\tilde{\tau}_0}\,, \tag{3.45}$$

where

$$G = \sqrt{1+\frac{g}{\Omega}} - 1\,.$$

For $g/\Omega \ll 1$ this gives back the previous result (3.41), while in the opposite limit $g/\Omega \gg 1$ one gets

$$g = \Omega(\tilde{\tau}+\tilde{\tau}_0)^2\,. \tag{3.46}$$

Importantly, for this solution the dropped term $\ddot{g}/\Omega$ is small compared to the other ones in (3.40) in both limits as long as $\Omega|G+1| \gg 1$. Therefore this solution provides a basis for a consistent $1/\Omega$ expansion which is valid everywhere apart in the small region $|G+1| \lesssim 1/\Omega$.

JHEP04(2009)118

Let us see what probability distribution one gets from the above solution. We can find $\tilde{\tau}_0(z)$ by imposing the boundary condition

$$f(0;z) = e^{-z} = e^{-g(\tilde{\tau}=0)}\,, \tag{3.47}$$

which gives

$$e^{\tilde{\tau}_0(x)} = Ae^A\,, \tag{3.48}$$

where we have defined

$$A \equiv \sqrt{1+x} - 1\,, \qquad x \equiv \frac{z}{\Omega}\,. \tag{3.49}$$

Then expression (3.8) for the probability distribution takes the following form

$$\rho(V,\tau) = \frac{\Omega}{2\pi i}\int_{0^+-i\infty}^{0^++i\infty} dx\, e^{-\Omega\left(G^2+2G-xV\right)}\,, \tag{3.50}$$

where G is a function of x via eqs. (3.45), (3.48) and (3.49). We can try to evaluate this integral using the saddle point approximation (we will check later whether this is a good approximation). The result reads

$$\rho(V,\tau) \approx \frac{\Omega}{\sqrt{2\pi|S''(x_0)|}} e^{-S(x_0)}\,, \tag{3.51}$$

where $S(x)$ is given by

$$S(x) = \Omega\left(G^2+2G-xV\right)\,, \tag{3.52}$$

and x_0 is the saddle point satisfying the equation

$$S'(x_0) = \Omega\left(2(1+G)G'\frac{\partial\tilde{\tau}_0}{\partial x} - V\right)\Big|_{x=x_0} = 0\,. \tag{3.53}$$

By taking the derivative of (3.45), and plugging in the resulting expression for G' into the saddle point condition (3.53) one gets

$$G = VA \tag{3.54}$$

at the saddle point. If we substitute this expression back in eq. (3.45) we get

$$Ge^G = AVe^{AV} = Ae^{\tilde{\tau}+A}\,, \tag{3.55}$$

$$\Rightarrow A = \frac{1}{V-1}\log\left(\frac{e^{3N_c}}{V}\right)\,. \tag{3.56}$$

Note that for $V < V_c \equiv e^{3N_c}$ the value of A is positive and the saddle point is at real and positive z (see figure 9). On the other hand for $V > V_c$ the value of A is negative and the saddle point is located at negative z.[4] To understand when the saddle point

[4]This implies that for $V > V_c$ the saddle point corresponds to a value for the boundary condition z that is outside of the physical region $z > 0$. We are using the analytic continuation of the solution, as it is implicit in the definition of the inverse-Laplace transform of eq. (3.50).

JHEP04(2009)118

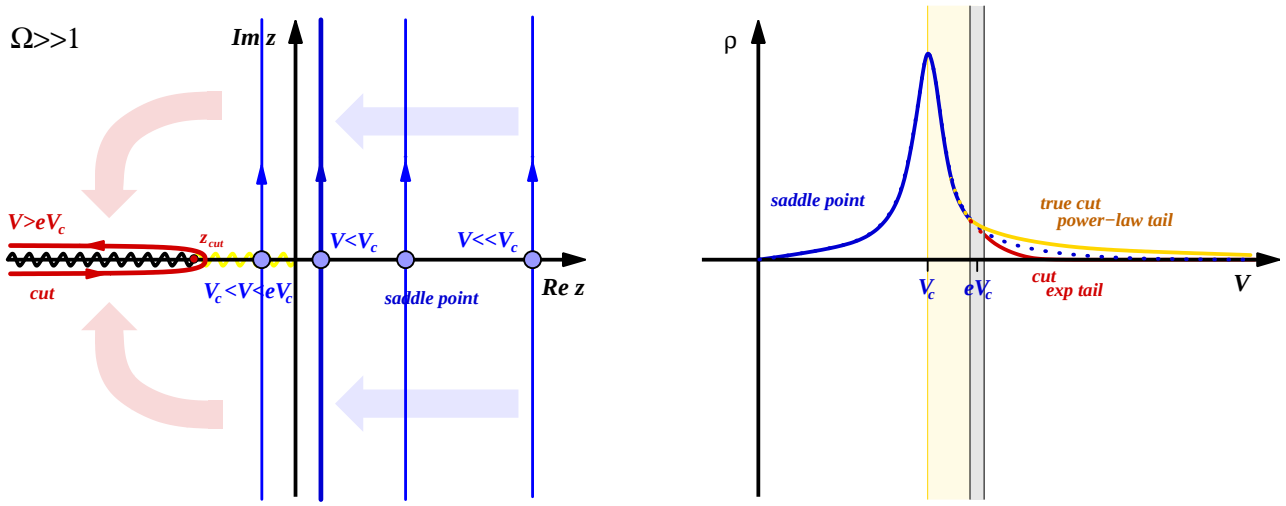

Figure 9. Contour of the anti-Laplace transform integral in the z-plane *(on the left)* and probability distribution of the volume *(on the right)* for $\Omega \gg 1$. For small volumes the integral can be solved via saddle-point approximation and gives a gaussian-like distribution *(in blue)*. Near $V = eV_c$ the saddle point hits the cut, the contour of integration can be deformed around the cut and for $V > eV_c$ the distribution becomes exponentially small *(in red)*. The large Ω limit does not capture the cut between $z_{\rm cut}$ and $z = 0$, which deforms the tail of the distribution (from a value of $V \in (V_c, eV_c)$ where $\rho(V) \approx e^{-\Omega}$) making it power-like in the volume *(in yellow)*.

approximation is applicable for calculating the integral (3.50) it is important to note that our approximate solution has a branch cut starting at the point $z_{\rm cut} \approx -2\Omega e^{-\tilde{\tau}-1}$, where $G = -1$ (equivalently, $g = -\Omega$). An easy way to see this is to use eq. (3.44) as an equation for $\partial g/\partial\tilde{\tau}$, namely

$$\frac{\partial g}{\partial \tilde{\tau}} = 2\Omega\left(-1 + \sqrt{1 + \frac{g}{\Omega}}\right) . \tag{3.57}$$

We see that at $g = -\Omega$ there is a discontinuity in the imaginary part of $\partial g/\partial\tilde{\tau}$ along the real axis in the g-plane at $g < -\Omega$, leading to a cut for g as a function of z at real $z < z_{\rm cut}$.

From (3.54) and (3.56) we find that the saddle point hits the cut at $V \simeq eV_c$. As long as the saddle point does not hit the cut, i.e. for $V \lesssim eV_c$, we can use the saddle point approximation to perform the integral. Plugging the solution in eqs. (3.54) and (3.56) back into S we get

$$S(x_0) = \Omega\frac{(V-1)}{V}G^2 = \Omega\frac{V}{V-1}\left[\log\left(\frac{V}{V_c}\right)\right]^2 , \tag{3.58}$$

$$S''(x_0) = \frac{\Omega(V-1)}{2}\left(1 - \frac{\log\left(\frac{V}{V_c}\right)}{V-1}\right)^{-1}\left(\frac{1}{V} - \frac{\log\left(\frac{V}{V_c}\right)}{V-1}\right)^{-1} , \tag{3.59}$$

and thus

$$\rho(V,\tau) \approx \mathcal{N} e^{-\Omega\frac{V}{V-1}\left[\log\left(\frac{V}{V_c}\right)\right]^2} , \qquad V \lesssim eV_c , \tag{3.60}$$

where the prefactor $\mathcal{N}$ is equal to

$$\mathcal{N} = \left|\frac{\Omega}{\pi V(V-1)}\left(1 - \frac{1}{V-1}\log\frac{V}{V_c}\right)\left(1 - \frac{V}{V-1}\log\frac{V}{V_c}\right)\right|^{1/2} .$$

JHEP04(2009)118

Notice that $S''(x_0)$ is large for exponentially large volumes, making our saddle point approximation justified.

For large volumes ($V \gg 1$) the formula (3.60) simplifies to

$$\rho(V,\tau) \sim \sqrt{\frac{\Omega}{\pi}\left|\log\frac{eV_c}{V}\right|}\frac{1}{V}\, e^{-\Omega\left(\log\frac{V}{V_c}\right)^2}\,, \qquad V \lesssim eV_c\,, \tag{3.61}$$

which we can also rewrite as the probability distribution to have N e-foldings

$$\tilde{\rho}(N,N_c) = 3V\rho(V,\tau) \sim 3\sqrt{\frac{\Omega|3N-3N_c-1|}{\pi}}\, e^{-\Omega(3N-3N_c)^2}\,, \qquad N \lesssim N_c\,. \tag{3.62}$$

This distribution is a gaussian centered around the classical number of e-foldings N_c (see figure 9). The spread is of order $1/\sqrt{\Omega}$ and goes to zero as Ω goes to infinity reproducing the δ-function of the classical limit.

When the volume becomes approximately eV_c the saddle point reaches the cut and we cannot perform the saddle point approximation anymore. In this regime, we can still close the contour of integration on the left around the cut (see figure 9), and perform the integral along the discontinuity. We obtain

$$\rho(V,\tilde{\tau}) = \frac{1}{2\pi i}\int_{|z_{\rm cut}|}^{+\infty} d|z|\; 2i\,\mathrm{Im}[f(\tilde{\tau};-|z|)]e^{-V|z|}\,. \tag{3.63}$$

It is straightforward to verify the $|f(\tilde{\tau};z)|$ does not grow faster than $e^{|z|}$ at large z. Therefore, at large volumes the integral above is dominated by values of z very close to the cut, with a spread of the order $1/V$. We can thus write approximately

$$\rho(V,\tilde{\tau}) \sim e^{z_{\rm cut}V} \sim e^{-2\frac{\Omega}{e}V/V_c}\,, \qquad V \gtrsim eV_c\,, \tag{3.64}$$

where we have ignored power corrections in the volume. We see that the probability distribution has an exponential tail in V that starts many standard deviations away from the average V_c. This result confirms that after the saddle point hits the cut one cannot use it any longer to evaluate the Laplace transform. Indeed, if one keeps using the saddle point approximation blindly one would obtain the gaussian behavior for the probability distribution up to arbitrary large volumes, in contradiction to (3.64).

However, there is a problem with the behavior (3.64) as well. Namely, this result disagrees with our analysis in section 3.1, where we found that high enough moments of the volume distribution diverge at any value of Ω. Related to this, we proved there that the function f has a cut starting at $z = 0$, while here we are finding the origin of the cut at $z = z_{\rm cut} < 0$.

The origin of this discrepancy is the non-commutativity of the large Ω limit and the large volume limit. One indication of the problem is that the large Ω expansion breaks in the vicinity of $G = -1$—precisely where the cut of the approximate solution starts. Even more relevant is the following observation. The leading non-analytic term in (3.17), that gives rise to the cut starting at $z = 0$, is proportional to $z^{4\Omega}$. At small z this term is non-perturbatively small in the large Ω expansion. However, it dominates the behavior

JHEP04(2009)118

of $\rho(V)$ at large volumes and gives rise to the power-law tail proportional to $V^{-4\Omega}$. Our approximate solution misses the corresponding part of the cut between 0 and $z_{\rm cut}$. Note, however, that this part of the cut becomes important only at volumes much larger than the average, where the probability is exponentially suppressed in Ω, $\rho(V) \propto e^{-\Omega}$. Consequently, our approximate solution correctly reproduces the shape of $\rho(V)$ up to $V \lesssim eV_c$. At larger volumes instead of the exponential behavior (3.64) one gets the power-law tail. In the next section we will discuss this tail in more details for general $\Omega > 1$.

3.3 $\Omega \geq 1$: approaching the phase transition

Let us now reconstruct the probability distribution of the volume for generic $\Omega \geq 1$. Unlike in the previous case, we do not have any small parameter that allows us to find an approximate full solution to the mechanical problem (3.1). However we will be able to find an approximate form of the probability distribution $\rho(V)$ practically at all V.

In order to do this, we notice that we can solve the differential equation (3.1) (and equivalently eq. (3.38)) in two different regimes. When $f \simeq 1$ (equivalent to $g \ll 1$), we can linearize the potential and obtain the solution

$$f_{\rm lin}(\tau; z) = 1 - e^{\omega_-(\tau+\tau_0)} - \sigma e^{\omega_+(\tau+\tau_0)}\,, \tag{3.65}$$

where $\omega_\pm \equiv \sqrt{\Omega} \pm \sqrt{\Omega - 1}$ and σ and τ_0 are integration constants. For the linear approximation to hold, it is enough to impose that $\tau + \tau_0 \ll -1$. Then, independently of the value of σ, for large enough $\tau + \tau_0$ we can approximate the solution as

$$f_{\rm lin} \approx 1 - e^{\omega_-(\tau+\tau_0)}\,. \tag{3.66}$$

The second regime in which we can solve the differential equation is when $f \simeq 0$ (equivalent to $g \gg 1$). In this regime the two dominant terms in (3.40) are those proportional to g and $(\frac{\partial g}{\partial \tau})^2$; by dropping the other terms one obtains

$$f \approx f_g = e^{-\frac{(\tau+\tau_1)^2}{4}}\,, \tag{3.67}$$

where τ_1 is an integration constant. By plugging this solution back into the equation, one may check that this approximation indeed holds as long as $g \gg 1$, i.e. for $|\tau + \tau_1| \gg 1$.

Notice that the constants of integrations in both cases can be absorbed into a shift (τ_0 or τ_1) of the "time" variable τ. τ_0 and τ_1 are in general not equal — they differ by an unknown constant of order one set by the matching of the two solutions. However, later we will be interested in the large $(\tau + \tau_0)$ limit where such a constant can be neglected and the τ_0 and τ_1 can be taken as equal.

Let us see now that this information is enough to reconstruct $\rho(V)$ almost for all V. First of all, we need to know how f depends on z. From section 3.1 (see eq. (3.17)), we know that $f(\tau; z)$ has a branch cut at $z = 0$. We could perform the integral by closing the contour around the cut, or by using the saddle point approximation. Let us start by seeing if and where we can use the saddle point approximation.

JHEP04(2009)118

For large volumes the saddle point is expected to lie at small z ($f \simeq 1$), where the exponential suppression in (3.8) is milder. In this case, near $\tau = 0$, the linearized approximation holds, and we can use $f_{\rm lin}$ to relate τ_0 to z. Next, in order to evaluate the integral (3.8), we need to impose that the saddle point belongs to one of the regions where our asymptotic solution works. Within the linearized regime there is no saddle point, so we will check whether the saddle point exists in the gaussian region at $\tau + \tau_0 \gg 1$.

Let us see how far the outlined procedure takes us and let us begin to implement it. Assuming that z at the saddle point is small (we will check this assumption later), we can determine τ_0 from the boundary condition

$$e^{-z} = f_{\rm lin}(\tau = 0; z) \approx 1 - e^{\omega_- \tau_0} \qquad \Rightarrow \qquad \tau_0 \approx \frac{1}{\omega_-} \log z \,. \tag{3.68}$$

We can now substitute this value for τ_0 in f_g and perform the integral (3.8) obtaining

$$\rho(V, \tau) \approx \frac{1}{\sqrt{2\pi |S''(z_0)|}} e^{-S(z_0)} \equiv \mathcal{N} e^{-S(z_0)} \,, \tag{3.69}$$

and $S(z)$ is given by

$$S(z) = \frac{1}{4} \left(\tau + \frac{1}{\omega_-} \log z \right)^2 - V z \,. \tag{3.70}$$

The saddle point condition $S'(z_0) = 0$ reads

$$\omega_- z_0 V = \frac{1}{2} \left(\tau + \frac{1}{\omega_-} \log z_0 \right) \qquad \Rightarrow \qquad z_0 \approx \frac{1}{2\omega_- V} \left[\tau - \frac{1}{\omega_-} \log \left(\frac{2\omega_- V}{\tau} \right) \right] . \tag{3.71}$$

We see that for relatively small volumes z_0 is positive and small, which justifies our assumption to use the linearized limit to match τ_0 with z. As V grows, z_0 moves towards zero (see figure 10) and reaches the region where the gaussian approximation breaks when $V \simeq \overline{V}$, with $\overline{V}$ given by

$$\overline{V} \equiv e^{\omega_- \tau} = e^{3N_c \frac{2}{1+\sqrt{1-1/\Omega}}} \,. \tag{3.72}$$

Even though we can not trust the gaussian approximation for $V \simeq \overline{V}$, we can try to follow the location of the saddle point, and we can see that it moves to negative values for $V \gtrsim \overline{V}$, reaching the location of the cut. This further justifies the approach we will take in the regime $V \gtrsim \overline{V}$, that is to do the integral along the cut.

For the moment instead let us concentrate on the regime of volumes $V \lesssim \overline{V}$, where we can apply the saddle point approximation. Substituting the value of the saddle point back into $S(z_0)$ we get

$$S(z_0) \approx \frac{1}{4} \left(\tau - \frac{1}{\omega_-} \log V \right)^2 = \Omega \left[3N_c - 3N \left(\frac{1 + \sqrt{1 - \frac{1}{\Omega}}}{2} \right) \right]^2 . \tag{3.73}$$

We see that $\tau + \tau_0$ at the saddle point is large whenever $S(z_0)$ is large, i.e. at large N and N_c as long as $N \lesssim 2(\Omega - \sqrt{\Omega(\Omega - 1)})N_c$, (compatibly with the condition $V \lesssim \overline{V}$), so that

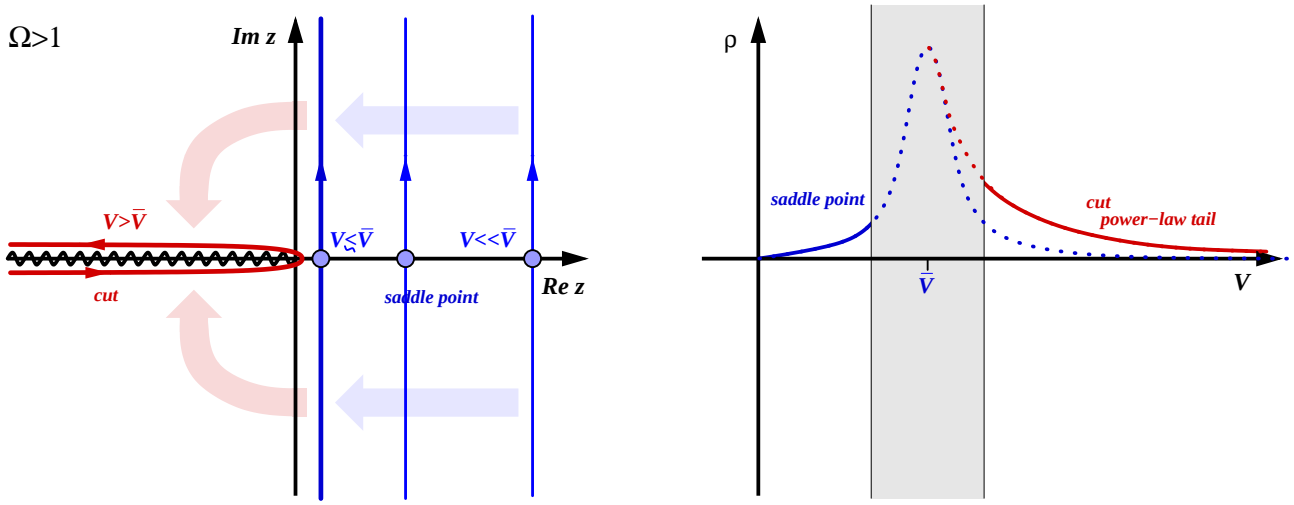

Figure 10. Contour of the anti-Laplace transform integral in the z-plane *(on the left)* and probability distribution of the volume *(on the right)* for $\Omega \gtrsim 1$. For small volumes the integral can be solved via saddle-point approximation and gives a gaussian-like distribution *(in blue)*. Around $V = \overline{V}$ *(gray region)* the saddle point hit the cut, which starts at $z = 0$, and our approximations for the solution of the differential equation break down. At larger volumes there is no saddle point anymore but the contour of integration can be deformed around the cut, giving a distribution tail that follows a power-law in the volume *(in red)*.

in the same regions we can trust the use of f_g for the saddle point. The corresponding value of $S''(x_0)$ is

$$S''(z_0) \approx \frac{2V^2(\sqrt{\Omega} - \sqrt{\Omega - 1})^2}{\log\left(\frac{V}{\overline{V}}\right)} \,. \tag{3.74}$$

As in the large Ω limit, $S''(x_0)$ is large for large volumes. So we conclude that the probability distributions for the volume after inflation for $V \lesssim \overline{V}$ and for generic $\Omega \geq 1$ has the form

$$\rho(V,\tau) \approx \mathcal{N} e^{-\frac{1}{4}\Omega\left(1+\sqrt{1-\frac{1}{\Omega}}\right)^2\left[\log\left(\frac{V}{\overline{V}}\right)\right]^2} = \mathcal{N} e^{-\Omega\left[\frac{3N}{2}\left(1+\sqrt{1-\frac{1}{\Omega}}\right)-3N_c\right]^2}, \qquad V \lesssim \overline{V}\,, \tag{3.75}$$

where in the last step we used that $3N = \log V$. We can trust this expression as long as $\log \overline{V} \gtrsim N \gg 1$ (see figure 10).

Let us now deal with the regime $V \gtrsim \overline{V}$. In this case, we have seen above that the saddle point z_0 enters the region very close to zero where we can not trust anymore the gaussian approximation. In section 3.2, eq. (3.17), we saw that $f(\tau; z)$ has a branch cut at the point $z = 0$. Near the branch cut, for sufficiently small values of z, we can take the linear approximation $f_{\rm lin}(\tau; z)$, which reads

$$\begin{aligned} f_{\rm lin}(\tau; z) &= 1 - \left(1 - e^{-z}\right) e^{\omega_- \tau} - \sigma e^{\omega_+ \tau_0} \left(e^{\omega_+ \tau} - e^{\omega_- \tau}\right) \\ &\simeq 1 - z e^{\omega_- \tau} - \sigma z^{\frac{\omega_+}{\omega_-}} e^{\omega_+ \tau}\,, \end{aligned} \tag{3.76}$$

JHEP04(2009)118

where in the last line we have used the approximate solution $\tau_0 \approx \log(z)/\omega_-$ of eq. (3.68). It is important to keep in mind that σ does not depend on z, but it is only fixed by the boundary condition at $\tau \to +\infty$.

Since $\omega_+/\omega_- = \omega_+^2$ in general is not integer, from eq. (3.76) we see that $f_{\rm lin}(\tau; z)$ has a branch cut at $z = 0$. In the $\Omega \gg 1$ case we did not see this cut starting at $z = 0$ because, at large Ω, $\omega_+/\omega_- \simeq 4\Omega$. At small z, this is a singularity that appears only non-perturbatively in $1/\Omega$ and could not be seen in a perturbative expansion in $1/\Omega$ as we did in the previous section.

We can now perform the integral of the discontinuity along the cut. As in section 3.2, we have to compute the imaginary part of $f(\tau; z)$ along the cut and then integrate it

$$\rho(V, \tau) = \frac{1}{2\pi i} \int_0^{+\infty} d|z|\; 2i\, \mathrm{Im}[f(\tau; -|z|)] e^{-V|z|} \,. \tag{3.77}$$

Since $f(\tau; z)e^{Vz}$ rapidly decreases when the real part of z is negative, at large enough volumes there is an interesting regime where the integral is dominated by small values of z, such that we can perform the integral using the linearized expression for $f(\tau; z)$. In this regime we have

$$\mathrm{Im}[f_{\rm lin}(\tau; z)]_{\rm cut} \sim e^{\omega_+ \tau} z^{\frac{\omega_+}{\omega_-}} \,. \tag{3.78}$$

where we neglected order one coefficients. By performing the integral (3.77) we obtain

$$\rho(V, \tau) \sim \frac{1}{V} \left(\frac{\overline{V}}{V}\right)^{\frac{\omega_+}{\omega_-}} \quad \text{for} \quad V \gtrsim \overline{V} \frac{\omega_+}{\omega_-} \,, \tag{3.79}$$

where we used that $e^{\omega_- \tau} = \overline{V}$. The condition on the right, that determines how large the volume should be for this approximation to work, comes from imposing the validity of the linear approximation for $f(\tau; z)$. Indeed, the integral is dominated by values of z around $z_s = \frac{\omega_+}{\omega_-} \frac{1}{V}$. For the linearized approximation to work $f_{\rm lin}(z_s; \tau)$ should be close to one. By plugging in the value for z_s in the expression for $f_{\rm lin}$, we find

$$f_{\rm lin} - 1 \simeq \frac{\omega_+}{\omega_-} \frac{\overline{V}}{V} + \sigma \left(\frac{\omega_+}{\omega_-} \frac{\overline{V}}{V}\right)^{\frac{\omega_+}{\omega_-}} \,, \tag{3.80}$$

which implies that the integral on the cut is well approximated by the integral of the linear solution for $V \gtrsim \frac{\omega_+}{\omega_-} \overline{V}$.

Similarly to the classical limit, the distribution for $V \lesssim \overline{V}$ is a gaussian in the number of e-folding centered at $\overline{V}$ with still a quite narrow width, of order one e-folding. Our method does not allow to reconstruct $\rho(V)$ in the vicinity of the average, $\overline{V} \lesssim V \lesssim \overline{V}\omega_+/\omega_-$. Note, however, that close to the eternal regime ω_+/ω_- is of order one, so that this range of volumes is not big. On the other hand at large Ω, when ω_+/ω_- is also large, we were able to find the probability distribution up to $V \simeq e\overline{V}$, where $\rho(V)$ was already exponentially suppressed as $e^{-\Omega}$.

For $V \gtrsim \overline{V}\omega_+/\omega_-$ the tail of the distribution in V is power law,

$$\rho(V, \tau) \sim V^{-1-\frac{\omega_+}{\omega_-}} \sim V^{-\Omega\left(1+\sqrt{1-\frac{1}{\Omega}}\right)^2 - 1} \,.$$

This tail agrees with our results in section 3.1 on the divergence of the multipoles (3.19).

As a cross-check of these results note that they imply that the average volume after inflation is given by

$$\langle V \rangle \simeq e^{\frac{6N_c}{1+\sqrt{1-\frac{1}{\Omega}}}} = \overline{V}\,, \tag{3.81}$$

in agreement with the direct computations in section 3.1 (eq. (3.25)) and in the appendix (eq. (A.10)). We see that as Ω approaches the critical point the average number of e-foldings shifts from N_c in the limit $\Omega \to \infty$ to $2N_c$ in the $\Omega \to 1$ limit.

3.4 $\Omega \lesssim 1$: inside eternal inflation

We now begin to explore the regime of eternal inflation. As Ω crosses 1, the solution of eq. (3.1) changes its form. The behavior of $f(\tau; z)$ around $f \simeq 1$ is not overdumped anymore. As discussed before, the normalization of the probability distribution drops below 1 in this regime.

We would like to follow this transition carefully. To this purpose, we take $\Omega = 1-\epsilon$ with $0 < \epsilon \ll 1$ and study the volume probability distribution within the eternal inflation regime by expanding in ϵ. We will follow the same strategy as in the previous two subsections. We expect that the solution $f(\tau; z)$ has a branch cut in the complex z plane, which allows us to perform the inverse-Laplace transform either with a saddle point approximation, if the saddle point is away from the cut, or along the cut itself.

If we decide to apply the saddle point approximation, we can concentrate on large enough τ, so that the saddle point lies in the region $f \to 0$ where the solution is well approximated by

$$f_g(\tau; z) = e^{-\frac{(\tau+\tau_0)^2}{4}}\,, \qquad \tau + \tau_0 \gg 1\,, \tag{3.82}$$

(we will check later what is the corresponding range of volumes) and τ_0 can be determined in terms of z in the linearized regime (as long as $z \ll 1$, as we will check below). The linearized solution is now given by

$$f_{\rm lin}(\tau; z) = 1 - \sigma e^{\sqrt{\Omega}(\tau+\tau_0)} \cos\left(\sqrt{\Omega-1}(\tau+\tau_0)\right) \approx 1 - \sigma e^{\tau+\tau_0} \cos\left(\sqrt{\epsilon}(\tau+\tau_0)\right)\,. \tag{3.83}$$

Note the oscillatory behavior of this linearized solution. By rescaling the constant σ, the constant τ_0 can be chosen equal to that in eq. (3.82). τ_0 will be fixed below in terms of the initial condition z; the constant σ on the other hand is fixed by matching with the gaussian solution. Notice that, as before, σ does not depend on z. We do not know the explicit value of σ, but we can argue that $\sigma \sim \mathcal{O}(1)$. Indeed, the gaussian solution breaks down when $\tau + \tau_0 \sim \mathcal{O}(1)$, afterwards the solution will reach the linear regime in a time $\Delta\tau \sim \mathcal{O}(1)$; this means that the linear approximation breaks down when $\tau + \tau_0 \sim \mathcal{O}(1)$, implying $\sigma \sim \mathcal{O}(1)$.

Let us now start the computation by fixing the relation between τ_0 and z via

$$e^{-z} = f_{\rm lin}(0; z) = 1 - \sigma e^{\tau_0} \cos\left(\sqrt{\epsilon}\tau_0\right) \quad \Rightarrow \quad z \approx \sigma e^{\tau_0} \cos\left(\sqrt{\epsilon}\tau_0\right)\,, \tag{3.84}$$

which is valid as long as $\tau_0 \ll -1$. Since the solution f is constrained to be between 0 and 1, in particular we need that for all τ in $0 \le \tau \lesssim -\tau_0$

$$f_{\rm lin}(\tau; z) \le 1\,, \tag{3.85}$$

which gives the lower bound

$$\tau_0 \geq -\frac{\pi}{2\sqrt{\epsilon}}\,. \tag{3.86}$$

Let us now study the analytic structure of $f(\tau; z)$. Continuity in ϵ suggests that $f(\tau; z)$ has a branch cut at large enough negative z as before. As ϵ approaches zero the origin of this cut $z_{\rm cut}$ goes to $z = 0$ as well. To follow how $z_{\rm cut}$ depends on ϵ at small ϵ note that eq. (3.83) implies that $f_{\rm lin}(\tau; z)$ is a function of z through its dependence on τ_0, upon which it depends analytically. So, the only non-analyticity in z of $f(\tau; z)$ can come from a non-analyticity of $\tau_0(z)$. The boundary condition (3.84) tells us that $z(\tau_0)$ is analytic. In inverting this relationship, therefore, the only non-analyticity can arise if $dz/d\tau_0$ vanishes at some value of z,

$$0 = \frac{dz}{d\tau_0} = \frac{\sigma e^{\tau_0}\left(\cos(\sqrt{\epsilon}\tau_0) - \sqrt{\epsilon}\sin(\sqrt{\epsilon}\tau_0)\right)}{1 - \sigma e^{\tau_0}\cos(\sqrt{\epsilon}\tau_0)} = 0 \tag{3.87}$$

$$\Rightarrow \cos(\sqrt{\epsilon}\tau_0) - \sqrt{\epsilon}\sin(\sqrt{\epsilon}\tau_0) = 0$$

$$\Rightarrow \tau_0 \simeq -\frac{\pi}{2\sqrt{\epsilon}} - 1\,. \tag{3.88}$$

By plugging this value into (3.84), we obtain

$$z_{\rm cut} \simeq -\frac{\sigma\sqrt{\epsilon}}{eV_\epsilon}\,, \tag{3.89}$$

where we defined

$$V_\epsilon \equiv e^{\frac{\pi}{2\sqrt{\epsilon}}}\,. \tag{3.90}$$

With this in mind, we can begin to evaluate the probability distribution using the saddle point approximation. As in the previous section

$$\rho(V,\tau) \approx \frac{1}{\sqrt{2\pi|S''(z_0)|}} e^{-S(z_0)} = \mathcal{N} e^{-S(z_0)}\,, \tag{3.91}$$

$$S(z) = \frac{1}{4}\left(\tau + \tau_0\right)^2 - zV\,, \tag{3.92}$$

where the saddle point z_0 is determined by

$$S'(z_0) = \frac{1}{2}\left[\tau + \tau_0(z_0)\right]\tau_0'(z_0) - V = 0 \qquad \Rightarrow \qquad V = \frac{(\tau+\tau_0)e^{-\tau_0}}{2\sigma\left[\cos(\sqrt{\epsilon}\tau_0) - \sqrt{\epsilon}\sin(\sqrt{\epsilon}\tau_0)\right]}\,. \tag{3.93}$$

The above relationship implies that for volumes that are large but smaller than $\overline{V} = e^{\tau}$, τ_0 is large and negative, so that the linear approximation in (3.84) is justified. $\tau + \tau_0$ is also large and positive, so that we can trust the gaussian approximation for $f(\tau; z_0)$. As long as $\tau_0 \gtrsim -\pi/(2\sqrt{\epsilon}) = -\log V_\epsilon$, the denominator does not vanish, and τ_0 is approximately given by

$$\tau_0 \approx -\log V\,. \tag{3.94}$$

The condition that $\tau_0 \gtrsim -\log V_\epsilon$ then reads $V \lesssim V_\epsilon$. When plugged back into eq. (3.91) the above solution gives the same form for $\rho(V,\tau)$ as in the case $\Omega \geq 1$, namely

$$\rho \approx \mathcal{N} e^{-\frac{1}{4}(\tau - \log V)^2} \qquad \text{for} \qquad 1 \ll V \lesssim \text{Min}\{\overline{V},\, V_\epsilon\}\,, \tag{3.95}$$

where

$$\mathcal{N} = \frac{1+\sqrt{1-\frac{1}{\overline{V}}}}{2\pi}\sqrt{\log\left(\frac{V}{\overline{V}}\right)}\,. \tag{3.96}$$

There are two interesting cases: $\overline{V} \lesssim V_\epsilon$ and $\overline{V} \gtrsim V_\epsilon$. Let us start with the case $\overline{V} \lesssim V_\epsilon$. As V reaches $\overline{V}$, $\tau_0 + \tau$ becomes of order one, and we can not trust anymore the gaussian solution. For this reason, in exploring the regime $V \gtrsim \overline{V}$, analogously to what we did in the case of $\Omega \geq 1$, we close the contour along the cut in the negative real z axis (see figure 11), and perform the integral of the imaginary part of $f(\tau; z)e^{zV}$

$$\rho(V,\tau) = \frac{1}{2\pi i}\int_{z_{\rm cut}}^{+\infty} d|z|\; 2i\,\mathrm{Im}[f(\tau;-|z|)]e^{-V|z|}\,. \tag{3.97}$$

Because of the exponential suppression, the integral is dominated by $|z| \sim 1/V > |z_{\rm cut}|$ for $V < V_\epsilon$. In this regime, $|z| \gtrsim |z_{\rm cut}|$, and from eq. (3.84) we have $\tau_0 \sim \log(z/\sigma)$. The condition $|z| \sim 1/V$ amounts to $\mathrm{Re}[\tau_0] \sim -\log V$ (notice that $\mathrm{Im}[\tau_0] \simeq i\pi$). Therefore in this regime $\tau + \mathrm{Re}[\tau_0] \sim \log(\overline{V}/V) \lesssim -1$, and we can use the linearized approximation $f_{\rm lin}(\tau; z)$ for $f(\tau; z)$. The imaginary part of $f_{\rm lin}(\tau; z)$ on the negative z axis is rather complicated. However, we can approximate $\cos(\sqrt{\epsilon}(\tau + \tau_0))$ with a constant of order one. Then, the integral (3.97) can be estimated as

$$\rho(V,\tau) \sim \int_{z_{\rm cut}}^{+\infty} d|z|\;\; e^{\tau} z\, e^{-V|z|} \sim \frac{\overline{V}}{V^2}\,, \qquad \overline{V} \lesssim V \lesssim V_\epsilon\,, \tag{3.98}$$

where we ignored constants of order one. We see that in this interval of volumes $\rho(V, \tau)$ decreases as $1/V^2$, exactly matching the analogous regime we found for $\Omega \gtrsim 1$.

As V keeps increasing and becomes larger than V_ϵ, the solution to the boundary condition eq. (3.84), with $z \sim 1/V$, gives $\tau_0 \simeq -\pi/(2\sqrt{\epsilon}) = -\log V_\epsilon$. In this case, the integral on the discontinuity becomes dominated by the beginning of the cut, and we obtain

$$\rho(V,\tau) \sim \int_{z_{\rm cut}}^{+\infty} d|z|\;\; e^{\tau}\frac{1}{V_\epsilon}\, e^{-V|z|} \sim \frac{\overline{V}}{V_\epsilon}\frac{1}{V} e^{-\frac{\sigma}{e}\sqrt{\epsilon}V/V_\epsilon}\,, \qquad \overline{V} \lesssim V_\epsilon \lesssim V\,, \tag{3.99}$$

where again we have ignored constants of order one, and where we have used that $z_{\rm cut} \simeq -\sigma\sqrt{\epsilon}/(eV_\epsilon)$. For volumes larger than V_ϵ, $\rho(V, \tau)$ decreases exponentially (this exponential tail was also recently found in [32]).

Notice how the two solutions (3.98) and (3.99) glue together: for $V \lesssim V_\epsilon$, τ_0 decreases like $-\log V$ giving a $1/V^2$ behavior to $\rho(V)$; when the volume reaches $\sim V_\epsilon$, τ_0 freezes at a value $\sim (-\log V_\epsilon) = -\pi/(2\sqrt{\epsilon})$ and the exponential tail $(e^{-\frac{\sigma}{e}\sqrt{\epsilon}\,V/V_\epsilon})$ kicks in. Notice also that the point, where the exponential tail enters, goes to infinity for $\epsilon \to 0$ smoothly matching the result for $\Omega \geq 1$.

Let us now concentrate on the opposite regime. Namely, as ϵ increases leaving τ fixed, at some point V_ϵ becomes smaller that $\overline{V}$. In this case, for $V \lesssim V_\epsilon$, we still have the result of eq. (3.95). However, for larger V, τ_0 does not continue to decrease as $-\log V$, because in this case the denominator of eq. (3.93) goes to zero and determines the behavior of τ_0.

JHEP04(2009)118

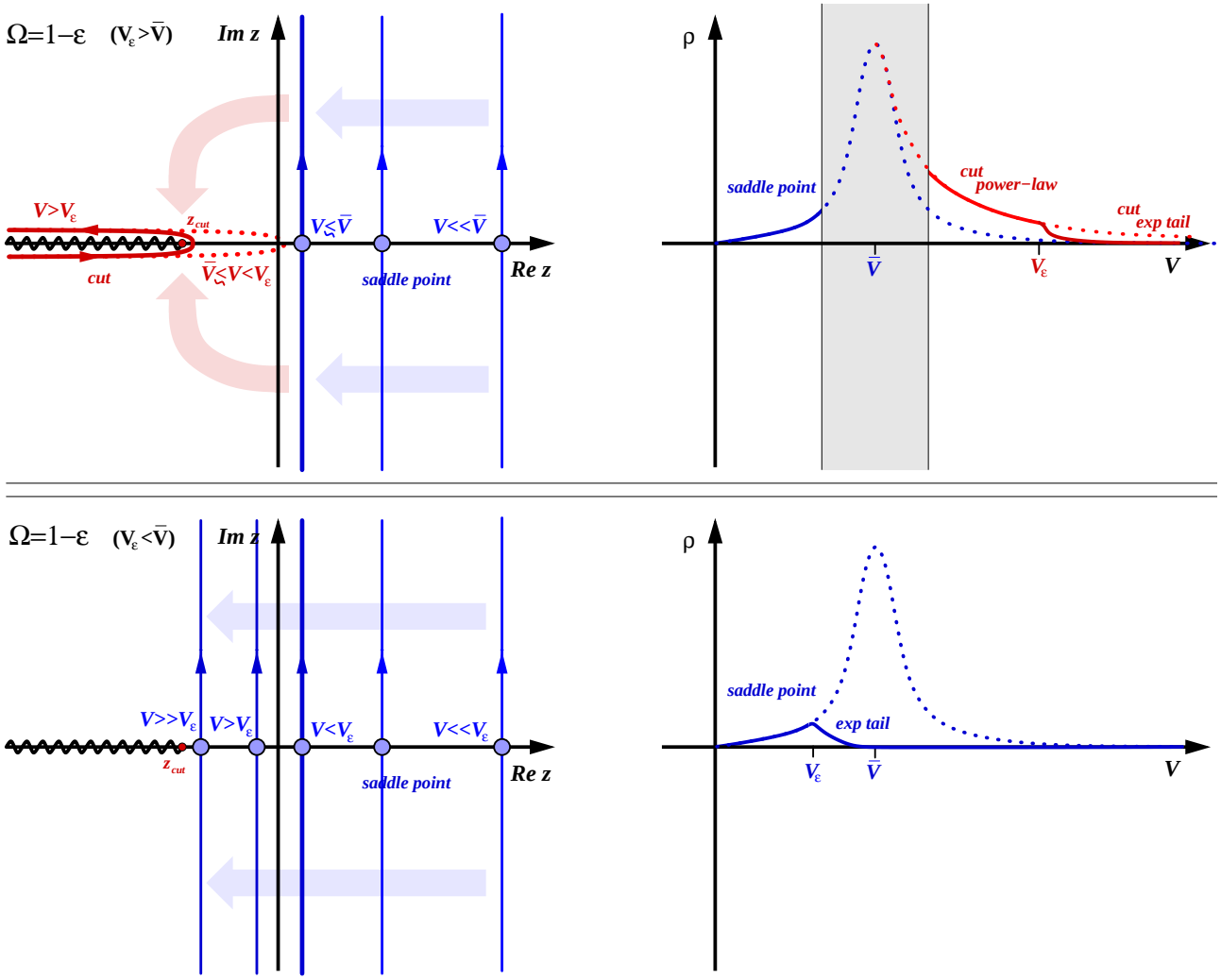

Figure 11. Contours of the anti-Laplace transform integrals in the z-plane *(on the left)* and probability distributions of the volume *(on the right)* for $\Omega = 1 - \epsilon$.

First case $\sqrt{\epsilon} < \pi/(2\tau)$ *(first row)*: at small volumes the integral can be solved via saddle-point approximation and gives a gaussian-like distribution *(in blue)*. Around $V = \overline{V}$ *(gray region)* our approximations for the solution of the differential equation break down. At larger volumes the contour of integration can be deformed around the cut. As long as $V \lesssim V_\epsilon$ the integral is dominated by a region that is much larger than the distance $z_{\rm cut}$ between the beginning of the cut and the origin, the integral is thus equivalent to the integral over a cut that starts at $z = 0$ *(dotted red contour)* giving a power-law behavior for $\rho(V, \tau)$ *(in light red)*. At $V \gtrsim V_\epsilon$, the contour integral "sees" the distance $z_{\rm cut}$ between the beginning of the cut and the origin, and it produces an exponential tail *(in dark red)*.

Second case $\sqrt{\epsilon} > \pi/(2\tau)$ *(second row)*: this time the saddle point works for all the volumes; for $V \lesssim V_\epsilon$ it produces a gaussian-like tail that is converted into an exponential tail for $V \gtrsim V_\epsilon$.

JHEP04(2009)118

In particular we can expand the denominator of eq. (3.93) around $\tau_0 = -\pi/(2\sqrt{\epsilon})$

$$2\sigma\left[\cos(\sqrt{\epsilon}\tau_0) - \sqrt{\epsilon}\sin(\sqrt{\epsilon}\tau_0)\right] \approx 2\sigma\sqrt{\epsilon}\left(\tau_0 + \frac{\pi}{2\sqrt{\epsilon}} + 1\right) , \tag{3.100}$$

that indeed vanishes for $\tau_0 = -\frac{\pi}{2\sqrt{\epsilon}} - 1$. We can now substitute eq. (3.100) into eq. (3.93) and get

$$\tau_0(z_0) \approx -\frac{\pi}{2\sqrt{\epsilon}} - 1 + \frac{e\left(\tau - \frac{\pi}{2\sqrt{\epsilon}}\right)}{2\sigma\sqrt{\epsilon}}\frac{V_\epsilon}{V} , \tag{3.101}$$

where the third term in the expression for τ_0 is small for $V \gg V_\epsilon$. We see that τ_0 approaches asymptotically from the positive side the value $\tau_0 = -\frac{\pi}{2\sqrt{\epsilon}} - 1$. In this regime, $\tau + \tau_0$ is always larger than one and positive, and the gaussian approximation to our solution holds. Further, by substituting (3.101) in (3.93), it is straightforward to see that z_0 moves on the real axis and approaches $z_{\rm cut}$ from the positive side, reaching $z_{\rm cut}$ only as $V \to \infty$. This tells us that for $V_\epsilon \lesssim \overline{V}$, unlike in all the former cases, the saddle point approximation holds for all V's. Plugging in the expression for the saddle point integral we get

$$\rho(V,\tau) \approx \mathcal{N} e^{-\frac{1}{4}\left(\tau - \frac{\pi}{2\sqrt{\epsilon}}\right)^2 - \frac{\sigma}{e}\sqrt{\epsilon}\, V/V_\epsilon} , \qquad V \gtrsim V_\epsilon , \tag{3.102}$$

with

$$\mathcal{N} = \frac{e^{3/2}}{\sqrt{8\pi\sigma\sqrt{\epsilon}}}\left(\frac{V_\epsilon}{V}\right)^{3/2}\frac{1}{V_\epsilon}\left|\log\left(\frac{\overline{V}}{V_\epsilon}\right)\right|^{3/2} . \tag{3.103}$$

We still have an exponential tail, with the same behavior as we found in the case in which $\overline{V}$ was smaller than V_ϵ. This is a very intuitive result: as ϵ increases, the exponential tails becomes relevant at smaller and smaller volumes, and it eats away the main part of the distribution (see figure 11). This also offers a consistency check between the two ways in which we are computing the inverse Laplace-transform: the saddle point approximation and the integral along the cut.

Finally the normalization of $\rho(V,\tau)$ changes smoothly when crossing the critical point $\Omega = 1$

$$P_{\rm ext} = f(\tau;0) \approx 1 - \sigma\sqrt{\epsilon}\,\tau\, e^{\tau - \frac{\pi}{2\sqrt{\epsilon}}} = 1 - 6\sigma\sqrt{\epsilon}N_c\frac{e^{6N_c}}{V_\epsilon} . \tag{3.104}$$

In the limit $\epsilon \to 0$ the normalization goes to one, but when the exponential tail starts to remove the bulk of $\rho(V,\tau)$ (i.e. $V_\epsilon \sim \langle V\rangle|_{\Omega=1} = e^{6N_c}$) the volume normalization quickly drops to 0.

For $\epsilon = \mathcal{O}(1)$ our approximations break down and the calculation becomes more complicated: the bound on τ_0 in eq. (3.86) becomes of $\mathcal{O}(1)$ and both the saddle-point approximation and the integral along the cut are dominated by the region of z where the linearized approximation no longer applies. However we can still say something about the normalization of the volume distribution $P_{\rm ext}$. For large τ the solution will still be in the gaussian regime, and we can write $f(\tau;z)$ as

$$f(\tau;z) = k(\Omega,z)e^{-\frac{(\tau+\tau_0(\Omega,z))^2}{4}} , \tag{3.105}$$

JHEP04(2009)118

where k and τ_0 are unknown constants that depend on Ω and z. From eq. (3.10) we know that

$$P_{\rm ext} = \int_0^\infty \rho(V)dV = f(\tau;0) = k(\Omega,0)e^{-\frac{(\tau+\tau_0(\Omega,0))^2}{4}} \ . \tag{3.106}$$

This formula does not tell us the explicit dependence on Ω of $P_{\rm ext}$ but since $\tau = 6N_c\sqrt{\Omega}$, we can extract the dependence of $P_{\rm ext}$ on the classical number of e-foldings N_c (equivalent to the initial position of the inflaton). For large N_c we get

$$P_{\rm ext} \sim e^{-\Omega(3N_c)^2} = e^{-\Omega(\log V_c)^2} \ . \tag{3.107}$$

The probability not to eternally inflate when $\Omega < 1$ goes to 0 exponentially with the square of the classical number of e-foldings.

Finally, note that the exponential behavior of $\rho(V)$ at $V > V_\epsilon$ implies that the moments of the distribution $\rho(V)$ do not diverge at $\Omega < 1$. Naively, this disagree with the results of [16]. However, there is no conflict. The point is that here we calculate moments using the probability distribution $\rho(V)$ obtained by taking the infinite time limit. At $\Omega < 1$ its normalization is less than one, indicating that there is a contribution localized at infinity that is not taken into account (cf. with the discussion of the two-site example in section 2.1.1). On the other hand, in the calculation of [16] one first finds the moments and only then takes the infinite time limit. The latter procedure effectively takes into account the contribution at infinity producing diverging moments at $\Omega < 1$.

3.5 $\Omega = 0$: Deeply inside eternal inflation

We are finally led to study the extreme limit of eternal inflation: the case $\Omega = 0$, which corresponds to a completely flat inflationary potential.

The job is quite easy in this case: the differential equation for f simplifies and we can find an explicit solution. With vanishing Ω the solution to eq. (3.1) that stops on the top of the potential in an infinite time reads

$$f(\tau;z) = e^{\frac{1}{2}-\frac{1}{4}\left(\tau+\sqrt{2+4z}\right)^2} \ . \tag{3.108}$$

Then the probability distribution is

$$\rho(V,\tau) = \frac{1}{2\pi}\int_{0^+-i\infty}^{0^++i\infty} dz\, e^{\frac{1}{2}-\frac{1}{4}\left(\tau+\sqrt{2+4z}\right)^2+zV} \ , \tag{3.109}$$

and to evaluate this integral we can use the saddle point method as before (actually, since the integral is gaussian in $\sqrt{2+4z}$, this procedure is exact).

The saddle point condition in this case reads

$$S(z) = -\frac{1}{2} + \frac{1}{4}\left(\tau+\sqrt{2+4z}\right)^2 - zV \ , \tag{3.110}$$

$$\Rightarrow \quad S'(z_0) = -V + \left(\frac{\tau}{\sqrt{2+4z_0}}+1\right) = 0 \ , \tag{3.111}$$

$$\Rightarrow \quad z_0 = \frac{\tau^2}{4(V-1)^2} - \frac{1}{2} \ , \tag{3.112}$$

so that

$$S(z_0) = \frac{V}{(V-1)}\frac{\tau^2}{4} + \frac{V-1}{2}\,, \tag{3.113}$$

$$S''(q_0) = \frac{2(1-V)^3}{\tau^2}\,, \tag{3.114}$$

and the expression for the probability distribution is

$$\rho(V,\tau) = \frac{\tau}{\sqrt{4\pi}(V-1)^{3/2}} e^{-\frac{V-1}{2} - \frac{V}{(V-1)}\frac{\tau^2}{4}}\,. \tag{3.115}$$

The tail of the distribution is again exponential, and this nicely matches the $\Omega \leq 1$ case we studied before.

We can easily also calculate the normalization for $\rho(V,\tau)$,

$$\int_0^\infty dV \rho(V,\tau) = e^{-\frac{\tau^2}{4} - \frac{\tau}{\sqrt{2}}} = f(\tau;0)\,, \tag{3.116}$$

which matches with the approximate formula of the previous section. As long as $\Omega \ll 1$ the corrections from the friction term in the differential equation are small, so that eq. (3.115) is a good approximation in this regime.

3.6 Realistic models: finite barrier effects and slow roll corrections

So far, we worked in the approximation of an infinitely long inflaton potential and treated Ω and H as constants. In a realistic situation both these assumptions do not hold: Ω and H change slowly as functions of the inflaton field and the latter can vary only in a finite range. This may be, for example, a consequence of either quantum gravity effects, if the potential grows monotonically up to high values of the field, or a reheating region if the potential has a maximum, or the steepening of the potential itself at a certain region. Let us discuss at the qualitative level how these effects change our results.

Let us begin with the consequences of the finite range of the inflaton field. The details of the underlying physical mechanism are not relevant for our qualitative discussion, so we introduce this effect by including a reflecting barrier in the stochastic process at large values of the inflaton field. In terms of the mechanical problem this implies that we are now looking for a solution that stops at a finite time τ_b (see (3.6)).

The presence of a barrier affects our results in two different ways: it changes the tail of the probability distribution and it slightly shifts the critical value Ω_c for the transition to the eternal regime. Let us start with the first effect. In the non-eternal regime, we have seen that the probability distribution is peaked around a volume of order $e^{3\overline{N}}$, where $\overline{N}$ is given by (1.6) and changes between N_c for large Ω and $2N_c$ at the transition point $\Omega = 1$. Given the relation $N_c = \tau/(6\sqrt{\Omega})$ this implies that the typical trajectory undergoes field excursions at most of order τ up the inflaton potential. Hence putting a barrier at τ_b does not affect the bulk of the trajectories, and therefore the probability distribution as long as the barrier is far enough from the starting point $\tau \ll \tau_b$. Still, the barrier cuts the trajectories that would have otherwise crossed it, and therefore we expect an additional

JHEP04(2009)118

suppression of the tail of the distribution for volumes corresponding to $\tau \gtrsim \tau_b$, that is for $N \gtrsim N_b$, where $N_b \equiv \tau_b/(6\sqrt{\Omega})$.

As a result, for $N > N_b$ the probability distribution becomes exponentially suppressed as a function of the volume as opposed to the $V^{-1-\omega_+/\omega_-}$ behavior that we found. There are several ways to see that the barrier indeed leads to the exponential suppression. For instance, as we saw in section 3.1, the function $f(z)$ is analytic at $z = 0$ when the barrier is present. Consequently, the whole integration contour for the Laplace transform can be deformed in the region with $\mathrm{Re}(z) < 0$, and at the large volumes the integral in (3.8) decays as $e^{-\mathrm{Re}(z_{\mathrm{cut}})V}$, where z_{cut} is the singularity of the function f at the smallest distance from the real axis.

In fact, recently an exponential tail of the volume distribution in the eternal regime was calculated in [32]. By extending the analysis of [32] into the non-eternal regime we verified that, as a result, the exponential suppression sets in for a number of e-foldings of order N_b. We do not provide details of this analysis here, as it would require an extensive introduction into methods of [32] and would take us too far away from the main line of our paper (instead, in the concluding section 4, we will present an intuitive argument explaining the origin of this exponential behavior). This also agrees with what we found in the two site models, where the probability distribution decreases exponentially at large volumes both in the eternal and the non-eternal regime.

Notice that, since $\Omega > 1$ implies $N_c < S_{\mathrm{dS}}/12$ (see eq. (1.4)), in the same regime we also have an upper bound on N_b, which has to satisfy the same condition $N_b < S_{\mathrm{dS}}/12$. This also means that the behavior of $\rho(V)$ for volumes larger than $e^{S_{\mathrm{dS}}/2}$ is always exponential in the volume, i.e. $\sim e^{-\mathrm{const}V}$. This property of the probability distribution will be further discussed in the next section in connection with the bound on the number of e-foldings.

The second effect of the barrier is related to the first. The presence of the barrier cuts out some of the trajectories producing the largest volumes and thus may slightly delay the entrance in the eternal regime to $\Omega_c < 1$. This shift can be calculated in the following way. Since Ω_c is defined as the value of Ω where P_{ext} starts deviating from one, and since $P_{\mathrm{ext}} = f(\tau; 0)$, we need to study the solution f for $z \to 0$. Consider some fixed $\Omega < 1$, and let us recall that in this case the oscillator is not anti-over-damped (eq. (3.1)). Around $f = 1$, we can linearize the potential and obtain an oscillating solution with a period

$$T = \frac{2\pi}{\sqrt{1-\Omega}}\,, \tag{3.117}$$

independently of the initial velocity, as the oscillations are harmonic (see the dotted lines of figure 7b). Consequently, in the linear regime it takes an amount of time equal to $T/4$ for the solution to come at rest. The returning force for the actual unharmonic potential (3.11) is smaller than for the corresponding harmonic potential, so it always takes longer than $T/4$ to come at rest (and can take arbitrarily long, as at $\Omega < 1$ there exists a solution that stops at the top of the hill in an infinite time). Consequently, if the barrier is close enough, $\tau_b < T/4$, there is no solution with the appropriate boundary condition, $\dot{f}(\tau_b; 0) = 0$ (except the trivial solution $f(\tau; 0) = 1$), even at $\Omega < 1$ and inflation is not eternal. This argument

JHEP04(2009)118

implies that the critical value for Ω is determined by

$$\tau_b = \frac{\pi}{2\sqrt{1-\Omega_c}} \quad \Rightarrow \quad \Omega_c = 1 - \left(\frac{\pi}{2\tau_b}\right)^2 . \tag{3.118}$$

Note that for $\Omega \lesssim \Omega_c$, the volume where the barrier effect sets in and changes the tail of the distribution is of order $V \lesssim V_b^2 = e^{6N_b} = e^{\pi/2\sqrt{1-\Omega_c}}$, that is always exponentially larger then the volume V_ϵ, where the exponential suppression found in section 3.4 sets in. Consequently, in the eternal regime the barrier affects only the tail of the distribution that is already suppressed as $e^{-\text{const}V}$.

Let us now discuss how the dependence of Ω and H on the inflaton field changes our results. Let us see first when this dependence become important. Throughout this paper we have been interested in what happens close to the eternal regime in the limit $M_{\rm Pl} \gg H$. In other words we have taken the limit $H/M_{\rm Pl} \to 0$, while keeping Ω fixed. This limit implies that we have been working in the extreme slow roll regime. Indeed, in this limit one has,

$$\frac{\dot{H}}{H^2} \sim \Omega \frac{H^2}{M_{\rm Pl}^2} \to 0 .$$

However, this does not imply that one can completely neglect the field dependence of Ω and H as we have another large parameter — the variation of the inflaton field or, equivalently, the number of e-foldings. For instance, by taking the variation of the Friedmann equation, one has

$$M_{\rm Pl}^2 H \Delta H \sim V' \Delta\phi$$

and the condition that H can be treated as a constant reads

$$\frac{\Delta H}{H} \sim \frac{V'\Delta\phi}{M_{\rm Pl}^2 H^2} \sim \Omega \frac{H^2}{M_{\rm Pl}^2} N_c \lesssim 1 . \tag{3.119}$$

So all our results apply if one takes the limit $H/M_{\rm Pl} \to 0$ while keeping Ω fixed and N_c small enough such that the inequality (3.119) holds. Note that (3.119) does not prevent us from considering arbitrarily large N_c if $H/M_{\rm Pl}$ is taken to be sufficiently small.

Nevertheless, one may wonder what happens to the shape of the volume probability distribution for longer inflaton trajectories, such that the variation of H (and Ω) has to be taken into account. In this case the coefficients in front of the different terms in the mechanical equation acquire a ϕ dependence [35]. This clearly may affect the details of the shape of the probability distribution. However, as long as $H \ll M_{\rm Pl}$ we still expect these effects to be small, with $\rho(V)$ still sharply peaked around the average number of e-foldings $\overline{N}$, which takes values between N_c and $2N_c$. One can check this statement by using the techniques of section 3.1 to calculate the average and the higher moments of the distribution. We can consider, for instance, the linear differential equation (3.21) for the average in the generic case, where Ω and H can be functions of the inflaton field ϕ (or equivalently of τ). In the variable τ, defined now as

$$\tau \equiv 6 \int \sqrt{\Omega} dN_c \, , \tag{3.120}$$

the differential equation for the average is the same as in eq. (3.21) with a small correction (of order $H^2/M_{\rm Pl}^2$) to the anti-friction term, which now depends on τ implicitly via Ω. Since in the non-eternal regime the anti-friction term is minimized at $\Omega = 1$, by setting $\Omega = 1$ we would obtain a trajectory that has a faster velocity at each moment of time in order to stop at the same moment as required by the boundary condition (3.23). It follows that the average is always smaller than e^τ, which, from eq. (1.3), is smaller than $e^{S_{\rm dS}/2}$. This implies that the bound $\overline{N} < S_{\rm dS}/6$ still holds.

In fact, we can also find an approximate expression for the average volume in the general case. Namely, for non-constant Ω, we can replace (3.25) by

$$\lim_{\tau_b \to \infty} \langle V \rangle = e^{\int \omega_- d\tau}, \tag{3.121}$$

which is a good approximate solution as soon as $\partial_\tau \Omega \ll \Omega$. This gives for the average number of e-foldings

$$3\overline{N} = \int \omega_- d\tau \,. \tag{3.122}$$

Analogous arguments can be applied for higher moments; as a result we see that the distribution remains peaked around the average value that takes value between N_c and $2N_c$.

4 Discussion

To summarize, in this paper we calculated explicitly the probability distribution $\rho(N)$ for the volume of the Universe after a period of slow-roll inflation (as before, by the number of e-foldings N we understand one third of the logarithm of the total volume produced during inflation, $N = \frac{1}{3}\log V$). Our results cover both the eternal and the non-eternal regime. Let us start this concluding section by summarizing these results and then by explaining how all different kinds of behavior we found for $\rho(N)$ have an intuitive physical explanation.

In general, the function $\rho(N)$ exhibits three qualitatively different regions. Namely, in the non-eternal regime $\Omega > 1$ it is peaked at $N \sim \overline{N}$, where the average number of e-foldings $\overline{N}$ is given by

$$\overline{N} = \frac{2N_c}{1 + \sqrt{1 - \Omega^{-1}}} \,. \tag{4.1}$$

For $N \lesssim \overline{N}$ it has a gaussian form,

$$\rho(N) \propto e^{-\frac{(3N - 3\overline{N})^2}{2\sigma^2}} \,, \tag{4.2}$$

with a width σ given by

$$\sigma^2 = \frac{2}{\Omega(1 + \sqrt{1 - \Omega^{-1}})^2} \,. \tag{4.3}$$

The behavior changes at $N \gtrsim \overline{N}$ where the probability distribution becomes exponential in N (or, equivalently, power-law in the volume V),

$$\rho(N) \propto e^{-6\Omega N\left(1+\sqrt{1-\frac{1}{\Omega}}\right)} = V^{-2\Omega\left(1+\sqrt{1-\frac{1}{\Omega}}\right)} \,. \tag{4.4}$$

JHEP04(2009)118

Finally, if a barrier preventing the inflaton to take arbitrary large values is present, this power-law tail becomes further suppressed at larger volumes and turns into an exponential in the *volume*

$$\rho(N) \propto e^{-ce^{3N}} = e^{-cV} \ . \tag{4.5}$$

This behavior sets in at $N \sim N_b$, where N_b is the number of e-foldings on the classical inflaton trajectory from the barrier till reheating.

What changes in the eternal regime, $\Omega < 1$, is that the exponential behavior (4.5) sets in at $N \simeq \pi/6\sqrt{1-\Omega}$ even if the barrier is absent. If $(1-\Omega)$ is not too small this happens at $N < \overline{N}$ so that the gaussian regime (4.2) interpolates directly to the superexponential one (4.5) without intermediate exponential behavior (4.4).

It is rather straightforward to understand the origin of the above three different types of behavior for $\rho(N)$ at the intuitive level. First, to produce a small number of e-foldings $N \ll N_c$, the inflaton field during the first few e-foldings needs to perform a jump in the whole volume to a value of ϕ corresponding to an average number of e-folding equal to N. The inflaton fluctuations away from the classical trajectory follow, at early times, a gaussian distribution (because of the random walk) and the size of the jump in field space is directly proportional to $(N - \overline{N})$, so the probability of such a jump is suppressed by $e^{-c(N-\overline{N})^2}$ (c is a constant) in agreement with our result (4.2) at small volumes.

On the other hand, the least expensive way to produce a large number of e-foldings $N \gg N_c$ is for one Hubble patch to go high up the potential, till values of the field corresponding to have a classical trajectory with N e-foldings. If such a fluctuation happened, the probability to produce at least N e-foldings becomes of order one. To estimate the probability of such a fluctuation, note again that the probability distribution for the inflaton fluctuations $\Delta\phi$ around the classical trajectory is gaussian. The crucial difference with the small volume case is that now it is not necessary for the fluctuation to happen in a short period of time, and the variance of the inflaton distribution grows linearly as a function of time t. As a result, the probability p of the fluctuation is maximized for times t corresponding to order N e-foldings, and depends exponentially on N, $p \propto e^{-c_1 \Delta\phi^2/t} \propto e^{-c_2 N}$ in agreement with (4.4). This argument is essentially identical to the one provided in [16] to explain why high enough moments of the volume distribution diverge in the non-eternal regime if no barrier is introduced.

The last argument fails at sufficiently large volumes both in the presence of a barrier at high values of the inflaton field and in the eternal regime. In the first case it fails because there is a limit on the maximum length of the classical trajectory, while in the second because even if a fluctuation to high values of the inflaton field happened, one is not guaranteed to end up with a *finite* number of e-foldings (in fact, the higher the fluctuation is the smaller is the probability for inflation to terminate). In both cases one ends up with getting a superexponential suppression of the probability distribution at large volumes, (4.5). This can roughly be explained by the necessity for an exponential number of independent and rather improbable events (corresponding to the individual Hubble volumes produced during inflation) to happen. Namely, in the eternal regime, inflation should terminate for $\sim e^{3N}$ Hubble patches and all their children (while in the

JHEP04(2009)118

non-eternal regime the probability for this to happen is equal to one). In the non-eternal case with a barrier, for $N \gg N_b$, an order $\sim e^{3N}$ Hubble patches have to live an anomalously long time, corresponding to a number of e-foldings much larger than N_b.

To summarize, we see that our results on the shape of the probability distribution of the reheating volume not only pass a number of consistency checks with results obtained by different methods, but also can be understood in a rather intuitive level. We believe making the explicit form of the volume probability available may help to understand the geometry of eternal inflation and offers also a natural "theoretical" observable that can be useful in further studies of eternal inflation.

A further motivation for doing our calculation was to establish whether a quantum version of the bound

$$3N \leq cS_{\rm dS} \ , \tag{4.6}$$

exists and, if so, whether this bound can be made sharp, i.e. whether there is a concrete value for the coefficient c in (4.6). Our results provide a positive answer to both questions. Namely, we find that the quantum version of the bound (4.6) can be formulated as follows:

The probability for slow-roll inflation to produce a finite volume larger than $e^{S_{\rm dS}/2}$, where $S_{\rm dS}$ is de Sitter entropy at the end of the inflationary stage, is suppressed below the uncertainty due to non-perturbative quantum gravity effects.

Indeed, our results imply that an inflaton trajectory with more than $2N_c$ e-foldings and such that inflation terminates globally in the entire space is exponentially unprobable, $\sim e^{-N}$. Given that in the non-eternal regime we have the bound (1.4), we conclude that the probability for slow-roll inflation to last more than $S_{\rm dS}/6$ e-foldings and to terminate globally in the entire space is smaller than the uncertainty coming from non-perturbative quantum gravitational effects ($\sim e^{-S_{\rm dS}}$). In fact, there is an even stronger statement that follows from the observation of section 3.6 about the bound on the barrier position N_b. Indeed, as long as $\Omega \gtrsim 1$, N_b is smaller than $S_{\rm dS}/12$, which implies that the transition to the regime where $\rho(V)$ drops exponentially with the volume ($e^{-{\rm const}\cdot V}$) starts exactly when the produced volume starts violating the bound, $V > e^{S_{\rm dS}/2} > e^{6N_b}$. Consequently, the probability to produce much larger volumes $V \gg e^{S_{\rm dS}/2}$ is super-exponentially suppressed, $\sim e^{-e^{S_{\rm dS}}}$. In turn this produces a super-exponentially small probability to produce volumes $V \gg e^{S_{\rm dS}/2}$.

We believe this provides a non-trivial test of the de Sitter complementarity idea. However, one may wish to go further and ask whether the particular value $c = 1/2$ that we found provides any insights into how the de Sitter complementarity works. Of course, all our calculations were done in the limit where gravity is non-dynamical, therefore it is not clear whether the value $c = 1/2$ really tells us something fundamental about the properties of de Sitter space. Let us however assume that it does and speculate on what would be the interpretation of this particular value. Recall that the original motivation for the bound (1.1) is coming from the idea that the black hole complementarity applies in the de Sitter case as well, so that the global effective field theory description of the FRW slices breaks down and information about the outside observers gets released in de Sitter fluctuations. Then, if inflation ends, there is the danger of violating the linearity of quantum

JHEP04(2009)118

mechanics by creating a "quantum xerox"—one can see the information twice, first holographically in the de Sitter fluctuations and later in a direct way when the corresponding mode comes in.

Recall that the analogous paradox could potentially arise in the black hole case after one measures more than $S_{bh}/2$ Hawking quanta (S_{bh} is the black hole entropy). In this case, the factor 1/2 arises because, as pointed out by Page [38], if one measures k degrees of freedom of a larger system described by n degrees of freedom, generically, the resulting density matrix looks thermal and carries less than a single bit of information as long as $k < n/2$.

This does not give rise however to any paradox: indeed, if one waits a long enough time outside the black hole, so that $\sim S_{bh}/2$ Hawking quanta are emitted, it is impossible to observe the same information a second time inside the black hole, since it gets destroyed by the curvature singularity.

It is tempting to interprete our result by saying that the de Sitter analogue of one Hawking quanta is produced every time a new Hubble patch is created from the volume where the observer lives (*i.e* every 1/3 of e-folding). Then the quantum-xerox problem would arise after $S_{\rm dS}/6$ e-foldings but it does not because of the bound.

Although it may sound quite natural, this interpretation raises a number of issues. First, as argued in [39], a single observer in *eternal* de Sitter can never run into the xerox paradox, as the largest amount of entropy that can be stored within a single causal patch is bounded by the Bekenstein area of the largest black hole that fits in a single patch. The latter is equal to $S_{\rm dS}/3$ and smaller than the minimal amount ($S_{\rm dS}/2$) required to extract the first bit of information.

However we are in a rather different situation here, as inflation eventually terminates. Therefore should the bound be not there, one would have the possibility to measure $S_{\rm dS}/4$ quanta, give them to a friend who leaves for a different Hubble patch, then measure other $S_{\rm dS}/4$ quanta and, after inflation ends, the two could meet and in this way collect $S_{\rm dS}/2$ quanta in total. Then the bound suggests that for the purpose of extracting information it is legitimate to collect quanta in one Hubble patch and keep them until the end of inflation in another. However, this reasoning also implies that it should not be possible to use quanta collected in *different* Hubble patches for extracting information — otherwise one would be forced to conclude that the actual bound on the number of e-folding is much stronger, $N \lesssim \log S$.

Notice also that if inflation does not terminate everywhere, then there is no problem of duplication of information if one observer lasts in the inflationary phase for longer than $S_{\rm dS}/6$ e-foldings: when the observer undergoes reheating and enters the Minkowski phase she is never able to see all the rest of the de Sitter space.

Another puzzle with drawing the parallel between the factor 1/2 in our bound and the one in the Page argument is that, if there are n light species around then, likely, the rate of how fast the information gets released is proportional to the number of species (at least this is so in the black hole case). On the other hand our bound does not depend on n (it could if the light species are scalars but does not for other fields).

JHEP04(2009)118

Finally, it is worth mentioning yet another reason why one should be cautious in taking the value $c = 1/2$ too seriously. Namely, here we focused on slow-roll models of inflation. In the effective field theory language of [37] these correspond to the models where the inflaton perturbations have sound velocity c_s equal to one. The classical version of the bound (1.1) was proven in [22] for general inflationary models, including those with small c_s. In fact at small c_s the classical bound becomes even stronger, $N_c \lesssim c_s^5 S_{\rm dS}$. However the reason it arises is somewhat different. At small sound velocities the strong coupling regime, where the effective field theory breaks down, sets in always before the eternal inflation regime. So the bound (1.1) in this case follows from the requirement that the system is weakly coupled and the null energy condition is not violated. Consequently, at the present stage we cannot exclude the possibility of violating the bound in the strongly coupled regime, although this possibility appears highly unlikely.

To summarize, we proved the quantum version of the bound on how long slow-roll inflation can last without becoming eternal. The existence of such a bound (eq. (4.6)) provides non-trivial support to de Sitter complementarity ideas, while it is still unclear whether the value of the coefficient $c = 1/2$ appearing in the bound that we found has a definite physical meaning. Before finishing, it is worth stressing that we believe that, independently of the answer to the last question, explicit calculations providing a detailed quantitative understanding of the transition to the eternal inflation regime, like those we preformed in the current paper, have an independent value. Indeed, it appears to us that a detailed understanding of the geometry and the dynamics of the eternally inflating Universe might be an important step to reach a final verdict on the puzzling issues raised by the observation of the cosmic acceleration and the string landscape.

Acknowledgments

We would like to thank Paolo Creminelli for initial collaboration in this project. It is a pleasure to thank Nima Arkani-Hamed, Raphael Bousso, Willy Fischler, Ben Freivogel, Alan Guth, Shamit Kachru, Andrei Linde, Hong Liu, Juan Maldacena, Alberto Nicolis, Sonia Paban, Uros Seljak, Steve Shenker, Eva Silverstein, Lenny Susskind, Enrico Trincherini, Alex Vilenkin and Matias Zaldarriaga for stimulating discussions. The work of SD and LS is supported in part respectively by the National Science Foundation under Grants No. PHY-0455649 and PHY-0503584.

A Volume average from the inflaton stochastic equation

As a cross-check of the method used in the paper, derived from the bacteria model, in this appendix we present an alternative calculation of the average volume $\langle V \rangle$ directly from the inflaton equations. The result is an improvement of a very similar computation performed in [16]. By definition the average of the volume is given by

$$\langle V \rangle = \int_0^\infty dV \; V \rho(V, \phi) \; , \tag{A.1}$$

JHEP04(2009)118

where the adimensional variable V is the volume expressed in units of the initial volume. This reduces to compute

$$\langle V \rangle = \int_{t_0}^{\infty} dt\, e^{3Ht} p_r(t)\ , \tag{A.2}$$

where $p_r(t)$ is the probability that at a given point $\vec{x}$ the field reaches the reheating value ϕ_r at time t. By translational invariance this probability does not depend on the point $\vec{x}$. Now the problem is reduced to compute $p_r(t)$. The latter is related to the probability $P(\bar{\phi}, t)$ for the inflaton to have a value $\bar{\phi}$ at time t by

$$p_r(t) = -\frac{d}{dt} \int_{\phi_r=0}^{+\infty} d\bar{\phi}\ P(\bar{\phi}, t)\ . \tag{A.3}$$

$P(\bar{\phi}, t)$ can be found by solving the classic stochastic diffusion equation [10, 11, 34]

$$\partial_{\sigma^2} \tilde{P}(\psi, \sigma^2) = \frac{1}{2} \partial_{\psi}^2 \tilde{P}(\psi, \sigma^2)\ . \tag{A.4}$$

where $\tilde{P}(\psi, \sigma^2) \equiv P(\bar{\phi}, t)$ and

$$\psi \equiv \bar{\phi} - \phi - \dot{\phi} t \tag{A.5}$$

is a Gaussian field with variance σ^2 that grows linearly with time

$$\sigma^2 = \frac{H^3}{4\pi^2} t\,. \tag{A.6}$$

ψ represents the fluctuations around the classical motion and undergoes a random walk. In the case the inflaton lives in a infinitely long potential and the reheating point is at $\phi_r = 0$, the solution of (A.4) is given by

$$\tilde{P}(\psi, \sigma^2) = \frac{1}{\sqrt{2\pi\sigma^2}} \left(e^{-\frac{\psi^2}{2\sigma^2}} - e^{-8\pi^2 \frac{\dot{\phi}\,\phi}{H^3}} e^{-\frac{(\psi+2\phi)^2}{2\sigma^2}} \right)\ , \tag{A.7}$$

which implies

$$p_r(t) = \sqrt{2\pi} \frac{\phi}{(H\,t)^{3/2}} e^{-2\pi^2 \frac{(\phi + \dot{\phi}\, t)^2}{H^3 t}}\ . \tag{A.8}$$

We see that the integral in (A.2) converges only when

$$\Omega \equiv \frac{2\pi^2}{3} \frac{\dot{\phi}^2}{H^4} \geq 1\ . \tag{A.9}$$

This is the first signal that the system has entered the eternal inflation regime. For $\Omega \geq 1$, we can explicitly perform the integral in (A.2), to obtain:

$$\langle V \rangle = e^{-2\pi \left(\frac{2\pi\dot{\phi} + \sqrt{(2\pi\dot{\phi})^2 - 6H^4}}{H^2} \right) \frac{\phi}{H}} = e^{2\sqrt{6}\pi \left(\sqrt{\Omega} - \sqrt{\Omega - 1} \right) \frac{\phi}{H}} = \begin{cases} V_c\,, & \Omega \gg 1 \\ V_c^2\,, & \Omega \to 1 \end{cases}\ , \qquad \Omega \geq 1\ . \tag{A.10}$$

where

$$V_c \equiv e^{\sqrt{\frac{6\pi^2}{\Omega}} \frac{\phi}{H}}\ ,$$

is the volume in the classical limit. The result, which agrees with eq. (3.81), is plotted in figure 8, where we can see the singular behavior at $\Omega = 1$.

JHEP04(2009)118

References

[1] Supernova Search Team collaboration, A.G. Riess et al., *Observational Evidence from Supernovae for an Accelerating Universe and a Cosmological Constant*, *Astron. J.* **116** (1998) 1009 [astro-ph/9805201] [SPIRES].

[2] Supernova Cosmology Project collaboration, S. Perlmutter et al., *Measurements of Omega and Lambda from 42 High-Redshift Supernovae*, *Astrophys. J.* **517** (1999) 565 [astro-ph/9812133] [SPIRES].

[3] WMAP collaboration, D.N. Spergel et al., *First Year Wilkinson Microwave Anisotropy Probe (WMAP) Observations: determination of Cosmological Parameters*, *Astrophys. J. Suppl.* **148** (2003) 175 [astro-ph/0302209] [SPIRES]; *Wilkinson Microwave Anisotropy Probe (WMAP) three year results: implications for cosmology*, *Astrophys. J. Suppl.* **170** (2007) 377 [astro-ph/0603449] [SPIRES].

[4] A.H. Guth, *The Inflationary Universe: a Possible Solution to the Horizon and Flatness Problems*, *Phys. Rev.* **D 23** (1981) 347 [SPIRES].

[5] A.D. Linde, *A New Inflationary Universe Scenario: a Possible Solution of the Horizon, Flatness, Homogeneity, Isotropy and Primordial Monopole Problems*, *Phys. Lett.* **B 108** (1982) 389 [SPIRES].

[6] A.J. Albrecht and P.J. Steinhardt, *Cosmology for Grand Unified Theories with Radiatively Induced Symmetry Breaking*, *Phys. Rev. Lett.* **48** (1982) 1220 [SPIRES].

[7] A.H. Guth and E.J. Weinberg, *Could the Universe Have Recovered from a Slow First Order Phase Transition?*, *Nucl. Phys.* **B 212** (1983) 321 [SPIRES].

[8] N. Arkani-Hamed, S. Dubovsky, L. Senatore and G. Villadoro, *(No) Eternal Inflation and Precision Higgs Physics*, *JHEP* **03** (2008) 075 [arXiv:0801.2399] [SPIRES].

[9] A. Vilenkin, *The Birth of Inflationary Universes*, *Phys. Rev.* **D 27** (1983) 2848 [SPIRES].

[10] A.D. Linde, *Eternally Existing Selfreproducing Chaotic Inflationary Universe*, *Phys. Lett.* **B 175** (1986) 395 [SPIRES].

[11] A.D. Linde, *Eternal chaotic inflation*, *Mod. Phys. Lett.* **A 1** (1986) 81 [SPIRES].

[12] M.R. Douglas and S. Kachru, *Flux compactification*, *Rev. Mod. Phys.* **79** (2007) 733 [hep-th/0610102] [SPIRES].

[13] R. Bousso and J. Polchinski, *Quantization of four-form fluxes and dynamical neutralization of the cosmological constant*, *JHEP* **06** (2000) 006 [hep-th/0004134] [SPIRES].

[14] S. Weinberg, *Anthropic Bound on the Cosmological Constant*, *Phys. Rev. Lett.* **59** (1987) 2607 [SPIRES].

[15] J.M. Maldacena, *Non-Gaussian features of primordial fluctuations in single field inflationary models*, *JHEP* **05** (2003) 013 [astro-ph/0210603] [SPIRES].

[16] P. Creminelli, S. Dubovsky, A. Nicolis, L. Senatore and M. Zaldarriaga, *The Phase Transition to Slow-roll Eternal Inflation*, *JHEP* **09** (2008) 036 [arXiv:0802.1067] [SPIRES].

[17] G.W. Gibbons and S.W. Hawking, *Cosmological Event Horizons, Thermodynamics and Particle Creation*, *Phys. Rev.* **D 15** (1977) 2738 [SPIRES].

[18] S. Kachru, R. Kallosh, A. Linde and S.P. Trivedi, *de Sitter vacua in string theory*, *Phys. Rev.* **D 68** (2003) 046005 [hep-th/0301240] [SPIRES].

[19] N. Goheer, M. Kleban and L. Susskind, *The trouble with de Sitter space*, *JHEP* **07** (2003) 056 [hep-th/0212209] [SPIRES].

JHEP04(2009)118

[20] T. Banks, *More thoughts on the quantum theory of stable de Sitter space*, hep-th/0503066 [SPIRES].

[21] R. Bousso, B. Freivogel and I.-S. Yang, *Eternal inflation: the inside story*, *Phys. Rev.* **D 74** (2006) 103516 [hep-th/0606114] [SPIRES].

[22] N. Arkani-Hamed, S. Dubovsky, A. Nicolis, E. Trincherini and G. Villadoro, *A Measure of de Sitter Entropy and Eternal Inflation*, *JHEP* **05** (2007) 055 [arXiv:0704.1814] [SPIRES].

[23] D.A. Lowe, J. Polchinski, L. Susskind, L. Thorlacius and J. Uglum, *Black hole complementarity versus locality*, *Phys. Rev.* **D 52** (1995) 6997 [hep-th/9506138] [SPIRES].

[24] S.W. Hawking, *Breakdown of Predictability in Gravitational Collapse*, *Phys. Rev.* **D 14** (1976) 2460 [SPIRES].

[25] J.M. Maldacena, *Eternal black holes in Anti-de-Sitter*, *JHEP* **04** (2003) 021 [hep-th/0106112] [SPIRES].

[26] S.W. Hawking, *Information Loss in Black Holes*, *Phys. Rev.* **D 72** (2005) 084013 [hep-th/0507171] [SPIRES].

[27] G. 't Hooft, *The black hole interpretation of string theory*, *Nucl. Phys.* **B 335** (1990) 138 [SPIRES].

[28] L. Susskind, L. Thorlacius and J. Uglum, *The Stretched horizon and black hole complementarity*, *Phys. Rev.* **D 48** (1993) 3743 [hep-th/9306069] [SPIRES].

[29] N. Arkani-Hamed, P. Creminelli, S. Mukohyama and M. Zaldarriaga, *Ghost Inflation*, *JCAP* **04** (2004) 001 [hep-th/0312100] [SPIRES].

[30] S.L. Dubovsky and S.M. Sibiryakov, *Spontaneous breaking of Lorentz invariance, black holes and perpetuum mobile of the 2nd kind*, *Phys. Lett.* **B 638** (2006) 509 [hep-th/0603158] [SPIRES].

[31] C. Eling, B.Z. Foster, T. Jacobson and A.C. Wall, *Lorentz violation and perpetual motion*, *Phys. Rev.* **D 75** (2007) 101502 [hep-th/0702124] [SPIRES].

[32] S. Winitzki, *Reheating-volume measure for random-walk inflation*, *Phys. Rev.* **D 78** (2008) 063517 [arXiv:0805.3940] [SPIRES].

[33] S. Winitzki, *On time-reparametrization invariance in eternal inflation*, *Phys. Rev.* **D 71** (2005) 123507 [gr-qc/0504084] [SPIRES].

[34] A.A. Starobinsky, in: *Fundamental Interactions* MGPI Press, Moscow (1984) pg. 55; in: *Current Topics in Field Theory, Quantum Gravity and Strings,* Lecture Notes in Physics, H.J. de Vega and N. Sanchez eds., Springer, Heidelberg, Germany (1986) pg. 107.

[35] S. Winitzki, *The eternal fractal in the universe*, *Phys. Rev.* **D 65** (2002) 083506 [gr-qc/0111048] [SPIRES].

[36] K.B. Athereya and P.E. Ney, *Branching Processes*, Springer, Berlin, Germany (1972); T.E. Harris *The Theory of Branching Processes*, Springer, Berlin, Germany (1963).

[37] C. Cheung, P. Creminelli, A.L. Fitzpatrick, J. Kaplan and L. Senatore, *The Effective Field Theory of Inflation*, *JHEP* **03** (2008) 014 [arXiv:0709.0293] [SPIRES].

[38] D.N. Page, *Information in black hole radiation*, *Phys. Rev. Lett.* **71** (1993) 3743 [hep-th/9306083] [SPIRES].

[39] M.K. Parikh and J.P. van der Schaar, *Not One Bit of de Sitter Information*, *JHEP* **09** (2008) 041 [arXiv:0804.0231] [SPIRES].

JHEP04(2009)118